Chemokine receptor CXCR3 facilitates CD8+ T cell differentiation into short-lived effector cells leading to memory degeneration

Makoto Kurachi,[1,2,4,6] Junko Kurachi,[1] Fumiko Suenaga,[1,6] Tatsuya Tsukui,[1,6] Jun Abe,[1,6] Satoshi Ueha,[1,6] Michio Tomura,[1] Kei Sugihara,[1,2] Shiki Takamura,[5] Kazuhiro Kakimi,[3] and Kouji Matsushima[1,6]

[1]Department of Molecular Preventive Medicine, [2]MD Scientist Training Program, [3]Department of Immunotherapeutics (Medinet), Graduate School of Medicine, and [4]Center for NanoBio Integration (CNBI), The University of Tokyo, 7-3-1 Hongo, Bunkyo-ku, Tokyo 113-0033, Japan
[5]Department of Immunology, Kinki University Faculty of Medicine, 377-2 Ohno-Higashi, Osaka-Sayama-shi, Osaka 589-8511, Japan
[6]Japan Science and Technology Agency, Core Research for Evolutional Science and Technology, Chiyoda-ku, Tokyo 102-0075, Japan

Strength of inflammatory stimuli during the early expansion phase plays a crucial role in the effector versus memory cell fate decision of CD8+ T cells. But it is not known how early lymphocyte distribution after infection has an impact on this process. We demonstrate that the chemokine receptor CXCR3 is involved in promoting CD8+ T cell commitment to an effector fate rather than a memory fate by regulating T cell recruitment to an antigen/inflammation site. After systemic viral or bacterial infection, the contraction of CXCR3$^{-/-}$ antigen-specific CD8+ T cells is significantly attenuated, resulting in massive accumulation of fully functional memory CD8+ T cells. Early after infection, CXCR3$^{-/-}$ antigen-specific CD8+ T cells fail to cluster at the marginal zone in the spleen where inflammatory cytokines such as IL-12 and IFN-α are abundant, thus receiving relatively weak inflammatory stimuli. Consequently, CXCR3$^{-/-}$ CD8+ T cells exhibit transient expression of CD25 and preferentially differentiate into memory precursor effector cells as compared with wild-type CD8+ T cells. This series of events has important implications for development of vaccination strategies to generate increased numbers of antigen-specific memory CD8+ T cells via inhibition of CXCR3-mediated T cell migration to inflamed microenvironments.

CORRESPONDENCE
Kouji Matsushima:
koujim@m.u-tokyo.ac.jp

Abbreviations used: LM-OVA, *Listeria monocytogenes* expressing OVA; MFI, mean fluorescence intensity; MPEC, memory precursor effector cell; MZ, marginal zone; RP, red pulp; SLEC, short-lived effector cell; VV-OVA, vaccinia virus expressing OVA; WP, white pulp.

Activation, differentiation, and subsequent memory development of T cell are regulated by a complex array of TCR signals, co-stimulation, and inflammation (Kaech et al., 2002; Kaech and Wherry, 2007; Williams and Bevan, 2007). Although the mechanism is unclear, varied T cell outcomes may depend on signal intensity reception in individual cells (Kaech and Wherry, 2007; Harty and Badovinac, 2008). In particular, there is emerging and compelling evidence that the inflammatory signals (signal 3), after those through TCR and costimulatory molecules, are crucial in determining effector and memory CD8+ T cell fate. IL-12 and type I IFN are essential for clonal expansion, differentiation of effector CD8+ T cells (Cousens et al., 1999; Curtsinger et al., 2005; Thompson et al., 2006), and memory development (Xiao et al., 2009). IL-2 signaling during expansion is also essential for development of memory CD8+ T cells capable of mounting full secondary expansion (Williams et al., 2006). Although these signals optimize CD8+ T cell responses, excessive and/or prolonged exposure to inflammatory signals is detrimental to generation of potent memory CD8+ T cells. For example, limiting inflammatory cues during the early expansion phase blunts contraction of antigen-specific CD8+ T cells, resulting in a massive memory pool (Badovinac et al., 2002, 2004). The same research group also established that DC immunization, in the absence of overt inflammation, accelerates generation of antigen-specific memory CD8+ T cells (Badovinac et al., 2005; Pham et al., 2009). Recent advances in classification of

The Rockefeller University Press $30.00
J. Exp. Med. Vol. 208 No. 8 1605-1620
www.jem.org/cgi/doi/10.1084/jem.20102101

effector CD8+ T cell subpopulations suggest how early inflammatory stimuli influence relative frequency of effector- or memory-fated cells. Based on expression of CD127 and KLRG1, effector CD8+ T cells can be divided into at least two major subsets: (1) terminally differentiated short-lived effector cells (SLECs; CD127lo KLRG1hi); and (2) memory precursor effector cells (MPECs; CD127hi KLRG1lo; Joshi et al., 2007). Increased IL-12 and IL-2 signaling on activation accelerates differentiation of CD8+ T cells toward SLECs to compensate for diminished effector CD8+ T cell conversion to memory cells (Joshi et al., 2007; Kalia et al., 2010; Pipkin et al., 2010). This inflammatory stimuli-mediated effector cell commitment into SLEC fate in the early expansion phase is regulated by transcription factor expression. IL-12 promotes CD8+ T cell expression of T-bet and represses Eomes in a dose-dependent manner, leading to greater SLEC frequency (Takemoto et al., 2006; Joshi et al., 2007; Rutishauser and Kaech, 2010). Another pair of transcription factors, Blimp-1 and Bcl-6, are also involved in this process; CD8+ T cells capable of receiving prolonged IL-2 signals (CD25hi cells) express higher levels of Blimp-1 (Kalia et al., 2010), whereas MPECs express higher levels of Bcl-6, a key negative regulator of Blimp-1 (Kallies et al., 2009; Rutishauser et al., 2009; Crotty et al., 2010). These findings suggest that effector and memory CD8+ T cell fate decisions are largely dictated by inflammatory signal strength during the early expansion phase (Harty and Badovinac, 2008). But how the inflammatory stimuli-mediated CD8+ T cell developmental program is influenced by the anatomical microenvironment and what factors determine early phase distribution of antigen-specific CD8+ T cells in lymphoid tissues are unknown.

In general, T cell migration to inflammation site is governed in a complex manner by surface expression of chemokine receptors and specific ligands (Bromley et al., 2008). CXCR3, a receptor for the inflammatory chemokines CXCL9/Mig, CXCL10/IP-10, and CXCL11/I-TAC, is preferentially expressed on activated CD8+ T cells in addition to Th1 cells and is thought to play an important role in trafficking to inflammation site (Hancock et al., 2000; Liu et al., 2005). In fact, CXCR3−/− effector CD8+ T cells show a significant defect in migrating from peripheral blood to inflamed nonlymphoid tissues such as lung, liver, brain, and vagina (Hokeness et al., 2007; Fadel et al., 2008; Zhang et al., 2008; Nakanishi et al., 2009). In addition to chemotaxis, CXCR3 signaling may influence development of effector T cells because CD8+ T cells in receptor- or ligand-knockout mice have reduced proliferative and cytotoxic ability (Dufour et al., 2002; Whiting et al., 2004; Thapa and Carr, 2009; Rosenblum et al., 2010). Although bystander effects, caused by overall deficiency of CXCR3 or its ligands in vivo, at the level of inflammatory response, should be considered as part of these studies, it is also known that stimulation of CXCR3 could induce phosphorylation of TCR signaling molecules and association of CXCR3 and CD3ε subunit on the T cell surface (Dar and Knechtle, 2007; Newton et al., 2009), indicating a potential role of CXCR3 for a costimulatory molecule. Unlike other inflammatory chemokine receptors, moreover, high-level expression of CXCR3 is evident on memory CD8+ T cells even after resolution of the inflammatory response and could be used as a marker to predict recall efficacy of memory CD8+ T cells (Hikono et al., 2007; Kohlmeier et al., 2008). Interestingly, differential expression of CXCR3 is critically associated with functional capacity of memory CD8+ T cells. CXCR3lo memory CD8+ T cells have a highly activated phenotype and decline in number over time, whereas CXCR3hi memory CD8+ T cells have a resting (stable) phenotype and become a predominant population at a later stage (Hikono et al., 2007). In addition, expression of CXCR3 gradually decreases when CD8+ T cells are exhausted during chronic lymphocytic choriomeningitis virus infection or experience multiple rounds of antigen challenge (Wherry et al., 2007; Wirth et al., 2010). How CXCR3 influences differentiation of the antigen-specific memory CD8+ T cells is therefore of great interest. Using TCR transgenic CD8+ T cells lacking CXCR3 and models of acute systemic viral and bacterial infection, we show that CXCR3-mediated microdistribution of CD8+ T cells in spleen (priming site) controls strength of inflammatory stimuli received by CD8+ T cells during the early expansion phase, thereby regulating effector/memory balance.

RESULTS

Attenuated contraction of CXCR3−/− antigen-specific CD8+ T cells in response to infection

It is known that effector CD8+ T cells up-regulate a variety of chemokine receptors to track inflammation. Although expression of these receptors, such as CCR5, is transient, CXCR3 is known to be continuously expressed on antigen-experienced CD8+ T cells even in the steady-state memory phase (Hikono et al., 2007; Kohlmeier et al., 2008). In fact, after systemic infection with recombinant vaccinia virus expressing OVA (VV-OVA), antigen-specific CD8+ T cells uniformly express CXCR3 at day 7, and high-level CXCR3 expression on memory CD8+ T cells is evident at least 70 d later (Fig. 1 A). This raises an important question. How do antigen-specific memory CD8+ T cells form in the absence of CXCR3? To answer this, we used a dual adoptive transfer approach in which CXCR3 was absent solely in one population of donor OT-I cells (Fig. 1 B). Recipient mice (CD45.1+) received a 1:1 mixture of naive CXCR3−/− (CD45.2+) and WT (CD45.1+ CD45.2+) OT-I cells and were then infected with VV-OVA. Both CXCR3−/− and WT OT-I input cells showed similar naive phenotypes and distributed in the same manner after adoptive transfer (Fig. S1). As shown in Fig. 1 (C and D), robust expansion of CXCR3−/− OT-I cells was observed during the acute phase of infection (until day 7) and was indistinguishable from that of the WT OT-I cells. Surprisingly, after peak of expansion CXCR3−/− OT-I cells showed significantly attenuated contraction, whereas WT OT-I cells declined ordinarily, resulting in CXCR3−/− OT-I cells predominating in the antigen-specific memory CD8+ T cell population at the later time points (Fig. 1, C and D).

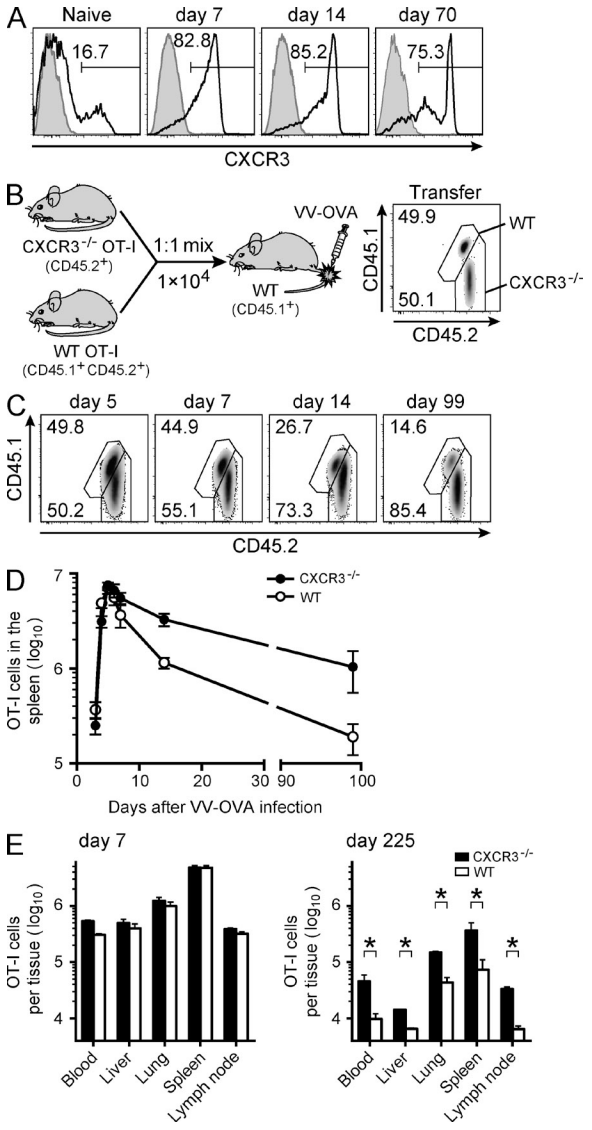

Figure 1. An increased number of CXCR3$^{-/-}$ memory CD8$^+$ T cells is observed in lymphoid and nonlymphoid organs. (A) Expression kinetics of CXCR3 on antigen-specific CD8$^+$ T cells in peripheral blood at the indicated times after VV-OVA infection. Representative histograms gated on CD8$^+$ T cells, CD44^{mid}, and CD62L^{lo} before infection and Kb-OVA$_{257}$–tetramer$^+$ after infection. Numbers on the plot indicate the percentage positive for CXCR3. Black line: CXCR3; shaded: isotype control. (B) Naive splenic CXCR3$^{-/-}$ (CD45.2$^+$) and WT (CD45.1$^+$CD45.2$^+$) OT-I cells were mixed in a 1:1 ratio, and a total of 1 × 10^4 cells were adoptively transferred into naive CD45.1$^+$ mice. The next day, the recipient mice were i.v. infected with 2 × 10^6 PFU VV-OVA. Flow plot shows representative mixed OT-I cells before transfer. (C) Representative plots gated on OT-I cells (CD45.2$^+$) in the spleen at the indicated times after infection. Numbers on the plots indicate the percentage of WT (top) and CXCR3$^{-/-}$ (bottom) OT-I cells in the total OT-I population. (D) Number of OT-I cells in the spleen after VV-OVA infection. Data are shown as mean ± SEM. (E) Number of OT-I cells in blood, liver, lung, spleen, and lymph nodes on day 7 (left) and day 225 (right) after infection. OT-I cells in blood are plotted per 1 × 10^7 cells. Data are shown as mean ± SEM. *, P < 0.05. Data represent two (A) or three (B–E) independent experiments (n = 4–5 and 3–4 per time point, respectively).

Increased frequency of splenic CXCR3$^{-/-}$ OT-I cells was not a result of the inability to migrate to nonlymphoid tissues because CXCR3$^{-/-}$ OT-I cells predominated in all lymphoid and nonlymphoid tissues in the memory phase (Fig. 1 E). Attenuated contraction of CXCR3$^{-/-}$ OT-I was not unique to vaccinia virus infection because increased frequency of CXCR3$^{-/-}$ memory OT-I cells was also observed after infection with recombinant *Listeria monocytogenes* expressing OVA (LM-OVA), both in dual and single adoptive transfer approaches (Fig. S2, A–D). Furthermore, to exclude potential impact of high precursor frequency on subsequent generations of antigen-specific memory CD8$^+$ T cells, we made mixed BM chimera in which irradiated C57BL/6 (B6) mice were reconstituted with BM from WT B6 mice and CXCR3-deficient donors (Fig. S2 E). As anticipated, after infection both populations of OVA$_{257-264}$–specific CD8$^+$ T cells expanded, at the same rate, to day 8, followed by sustained numbers of antigen-specific memory CD8$^+$ T cells lacking CXCR3 (Fig. S2, F and G). This supports our observation that CXCR3$^{-/-}$ CD8$^+$ T cells have preferential ability to form a memory CD8$^+$ T cell pool. Furthermore, using the same dual adoptive transfer approach we observed no difference in frequencies of CCR5$^{-/-}$ and WT OT-I cells throughout the response (Fig. S3), indicating that attenuated contraction of antigen-specific CD8$^+$ T cells is unique to cells lacking CXCR3, not CCR5. Altogether, we conclude that memory CD8$^+$ T cell formation in response to infection is significantly facilitated by absence of CXCR3.

CXCR3$^{-/-}$ and WT memory CD8$^+$ T cells show similar functional properties

Given the relative dominance of the CXCR3$^{-/-}$ memory CD8$^+$ T cell population compared with its WT counterpart, it is useful to compare their functional characteristics as potent providers of immune protection. Using the same dual adoptive transfer approach, we first evaluated their abilities to produce effector cytokines upon in vitro restimulation. As shown in Fig. 2 A, both memory OT-I cells had a similar ability to produce IFN-γ and TNF. However, the fraction of IFN-γ$^+$ cells that produced IL-2 in CXCR3$^{-/-}$ OT-I cells was higher than that in WT OT-I cells (Fig. 2, A and B). There appears to be an inverse correlation between activation status and ability of CD8$^+$ T cells to produce IL-2, such that cells with the rested (naive or memory) phenotype have superior ability to produce IL-2 in response to antigenic stimulation (Kaech et al., 2003; Wherry et al., 2003; Marzo et al., 2005; Intlekofer et al., 2007; Joshi et al., 2007; Sarkar et al., 2008). Consequently, WT OT-I cells may exhibit the characteristics of memory cells with highly activated status relative to CXCR3$^{-/-}$ OT-I cells. Increased expression of granzyme B protein in WT OT-I cells compared with CXCR3$^{-/-}$ OT-I cells also supports this hypothesis (Fig. 2 C).

Next, we compared their abilities to mount recall response on rechallenge. More than 40 d after infection, CD8$^+$ enriched spleen cells containing equivalent numbers of CXCR3$^{-/-}$ and WT OT-I cells were labeled with CFSE and transferred

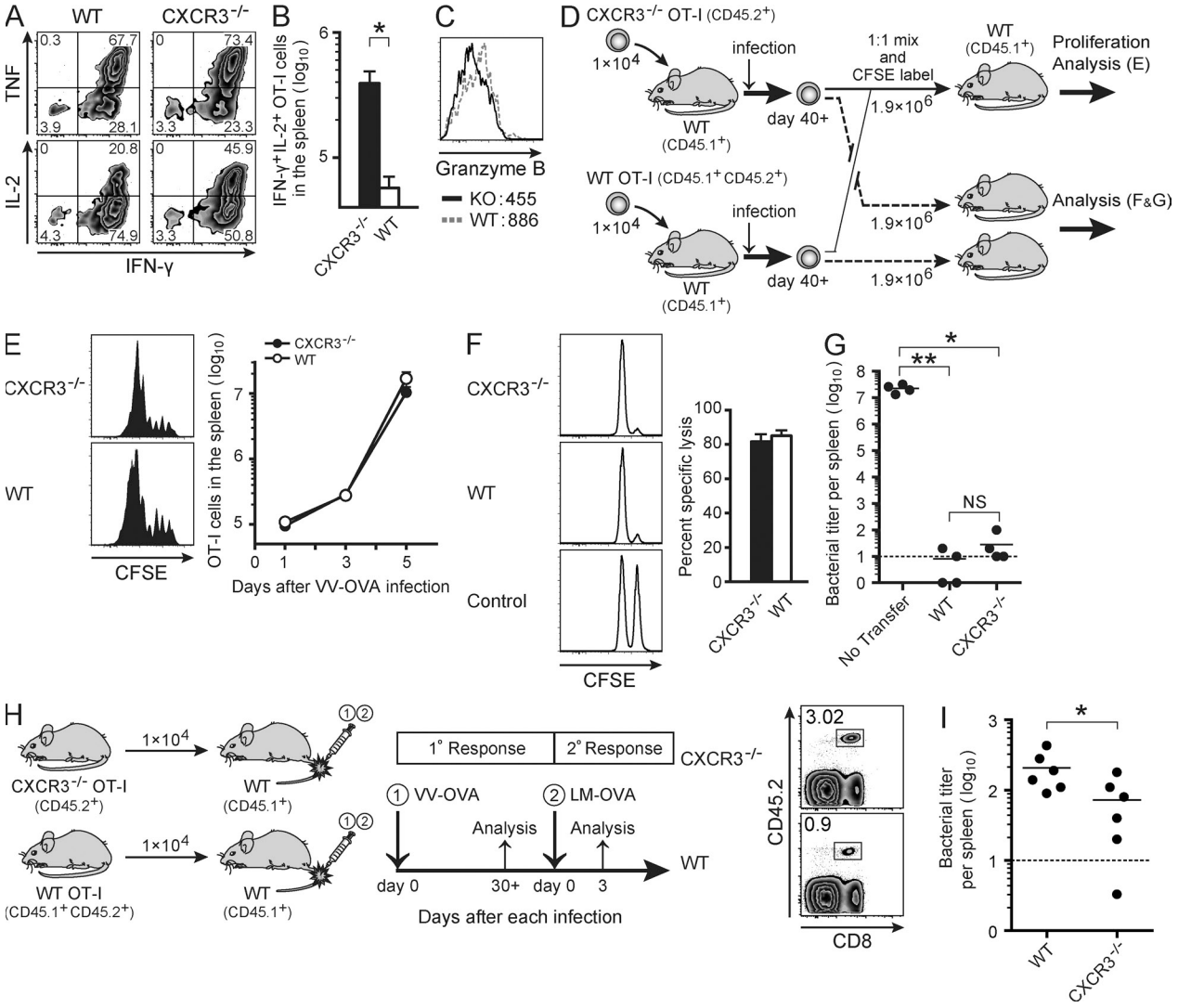

Figure 2. CXCR3$^{-/-}$ memory CD8$^+$ T cells exhibit similar functional capacities to WT cells. (A–C) Mixed CXCR3$^{-/-}$ and WT OT-I cells were transferred, followed by VV-OVA infection as in Fig.1 B. Cytokine production and granzyme B expression by CXCR3$^{-/-}$ and WT memory OT-I cells was analyzed at day 43 after infection. (A) Representative flow cytometry plots showing TNF, IL-2, and IFN-γ production. (B) Number of IFN-γ$^+$ IL-2$^+$ OT-I cells in the spleen. Data are shown as mean ± SEM. *, P < 0.01. (C) Granzyme B expression. Numbers below the granzyme B plots show mean fluorescence intensity (MFI). (D) CXCR3$^{-/-}$ or WT memory OT-I cells were generated in separate hosts and isolated from spleen at day 40+ after infection. CXCR3$^{-/-}$ and WT memory OT-I cells were CFSE labeled or not and adoptively transferred in a 1:1 mixture (1.9 × 10^6 cells total). (E) Recipient mice were rechallenged with VV-OVA 1 d after transfer. Representative plots showing proliferation of both OT-I cells on day 3 after infection as determined by CFSE dilution. Data are shown as mean ± SEM. (F) 1 d after transfer of unlabeled CXCR3$^{-/-}$ or WT memory OT-I cells, OVA peptide–pulsed (CFSE^{hi}) and unpulsed (CFSE^{lo}) target cells were injected and killing was assessed 4 h later. Data are shown as mean ± SEM. (G) 1 d after transfer of unlabeled memory OT-I cells, recipient mice were challenged i.v. with 1 × 10^6 CFU LM-OVA. Bacterial numbers in the spleen were determined 3 d after challenge. Bars represent mean. *, P < 0.001; **, P < 0.005. Data represent three (A–C) or two (D–G) independent experiments (n = 3–4 per time point). (H and I) 1 × 10^4 naive splenic CXCR3$^{-/-}$ or WT OT-I cells were transferred into separate CD45.1 WT recipients, followed by i.v. infection with 2 × 10^6 PFU VV-OVA. After day 30+, the recipient mice were challenged i.v. with 1 × 10^7 CFU LM-OVA. Data represent two independent experiments (n = 4–6 per group). (H) Flow cytometry plots show the frequency of CXCR3$^{-/-}$ or WT OT-I cells in PBMC 1 d before LM-OVA challenge. (I) Bacterial titers in the spleen at 3 d after challenge. Bars represent mean. *, P < 0.05.

into recipient mice (Fig. 2 D). 1 d later, recipient mice were infected with VV-OVA. As shown in Fig. 2 E, there were no differences in early proliferation and secondary expansion between CXCR3$^{-/-}$ and WT memory OT-I cells. To further investigate their abilities to confer protective immunity, we performed in vivo killing assay and found that, consistent with the previous findings, CXCR3$^{-/-}$ and WT memory OT-I cells exhibited similar ability to kill specific target cells in vivo (Fig. 2 F). After LM-OVA challenge, moreover, both CXCR3$^{-/-}$ and WT memory OT-I cells conferred equivalent protective immunity on a per-cell basis (Fig. 2 G). These results demonstrate that, despite slightly different cytokine profiles, both memory populations differentiate into equally potent killer cells after reactivation and confer similar protective immunity on a per-cell basis.

Given that the number of memory CXCR3$^{-/-}$ CD8$^+$ cells surpassed that of WT cells, we propose that increased generation of memory CD8$^+$ T cells by CXCR3 inhibition during initial immunization would confer superior protection at the whole-body level upon subsequent infection. To test this idea, we rechallenged CXCR3$^{-/-}$ and WT mice with LM-OVA, which had been immunized by VV-OVA (Fig. S4). As shown in Fig. S4 B, consistent with the results described in Fig. 1 and Fig. S2, CXCR3$^{-/-}$ mice exhibited an increased number of antigen-specific memory CD8$^+$ T cells. Importantly, compared with WT mice, these CXCR3$^{-/-}$ mice showed reduced bacterial burden after rechallenge (Fig. S4 C). To exclude the possibility that global CXCR3 deficiency might affect protection as a result of alteration of the overall inflammatory or immune response during rechallenge, we also examined pathogen titers in OT-I single-transferred mice in which CXCR3 deficiency is limited to antigen-specific CD8$^+$ T cells (Fig. 2, H–I). Consistent with observations in CXCR3$^{-/-}$ mice, the mice containing an increased number of CXCR3$^{-/-}$ memory OT-I cells showed enhanced protective immunity compared with WT memory OT-I cells. Collectively, these results suggest that CXCR3 blockade during immunization might be a useful strategy for improving the vaccine efficacy.

CXCR3$^{-/-}$ and WT memory CD8$^+$ T cells show similar proliferative ability

Next, we addressed how massive memory CD8$^+$ T cells form when T cells lack surface expression of CXCR3. First, by conducting tetramer binding assay and checking functional avidity, we excluded the possibility that altered differentiation of CXCR3$^{-/-}$ memory cells is a result of different TCR expression or TCR signaling between CXCR3$^{-/-}$ and WT cells (Slifka and Whitton, 2001). We found that CXCR3$^{-/-}$ OT-I cells express a similar level of TCR and produce a similar amount of IFN-γ with diluted concentration of cognate peptide stimulation (Fig. S5). We next hypothesized that CXCR3$^{-/-}$ memory CD8$^+$ T cells have superior capacity to persist long term in vivo and undergo higher homeostatic proliferation compared with WT memory CD8$^+$ T cells. To test this, we first compared the phenotypes of CXCR3$^{-/-}$ and WT memory CD8$^+$ T cells. As expected, CXCR3$^{-/-}$ memory OT-I cells contained more CD62L^{hi} CCR7^{hi} central memory cells (Fig. 3 A). Moreover, as shown in Fig. 3 (B–D), CXCR3$^{-/-}$ memory CD8$^+$ T cells also showed the characteristics of high memory potential compared with their WT counterparts, as determined by expression of CD127, KLRG1, CD27, and CD122 (Kaech and Wherry, 2007; Williams and Bevan, 2007; Rutishauser and Kaech, 2010), which is consistent with their cytokine profile upon restimulation (Fig. 2, A–C). These findings suggest that the skewed ratio of CXCR3$^{-/-}$ to WT memory CD8$^+$ T cells may be a consequence of superior homeostatic proliferation of CXCR3$^{-/-}$ memory CD8$^+$ T cells. To investigate this, mice were given BrdU during the memory phase, and frequency of BrdU$^+$ cells was then compared. We were surprised to observe no difference in BrdU incorporation between CXCR3$^{-/-}$ and WT memory CD8$^+$ T cells (Fig. 3 E). Transferring CFSE-labeled memory OT-I cells into naive mice without irradiation also confirmed this finding. 17 d later, the division profiles of CXCR3$^{-/-}$ and WT memory CD8$^+$ T cells revealed that

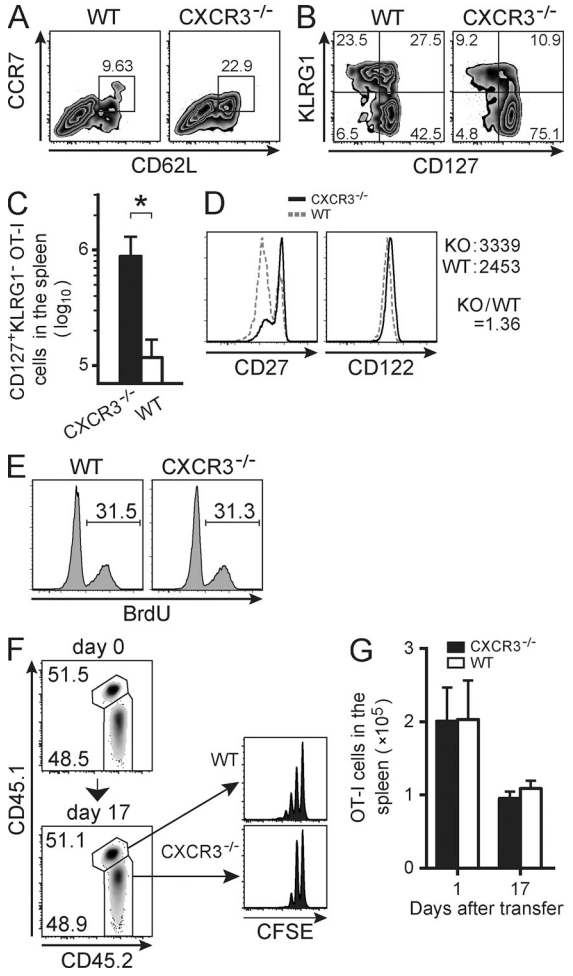

Figure 3. CXCR3$^{-/-}$ memory CD8$^+$ T cells display a high memory potential phenotype. (A–D) 1 d after transfer of mixed CXCR3$^{-/-}$ and WT OT-I cells, recipient mice were infected with VV-OVA as in Fig.1 B. (A and B) Surface expression of indicated markers on CXCR3$^{-/-}$ and WT OT-I cells in the spleen was analyzed on day 99 after infection. (C) Numbers of CD127^{hi} KLRG1^{lo} cells in the spleen at day 99 are shown as mean ± SEM. *, $P < 0.05$. (D) Expression of CD27 and CD122 on splenic OT-I cells at the same time point. Numbers to the right of the CD122 plots indicate the MFI and MFI ratio of CXCR3$^{-/-}$ to WT. (E) 70+ d after transfer, the recipient mice containing both CXCR3$^{-/-}$ and WT memory OT-I cells were administered BrdU for 17 d. (F and G) CXCR3$^{-/-}$ and WT memory OT-I cells were generated in separate hosts as shown in Fig. 2 D. On day 40+ after infection, OT-I cells were isolated from spleen, labeled with CFSE, and co-transferred into naive nonirradiated recipient mice. (F) Homeostatic proliferation was determined by CFSE dilution 17 d after transfer. Histograms gated on OT-I cells show the ratio of CXCR3$^{-/-}$ and WT OT-I cells at transfer (day 0) and day 17 after transfer, and CFSE dilution. (G) Number of OT-I cells in spleen. Data are shown as mean ± SEM. Data represent three (A–D) or two (E–G) independent experiments (n = 3–4).

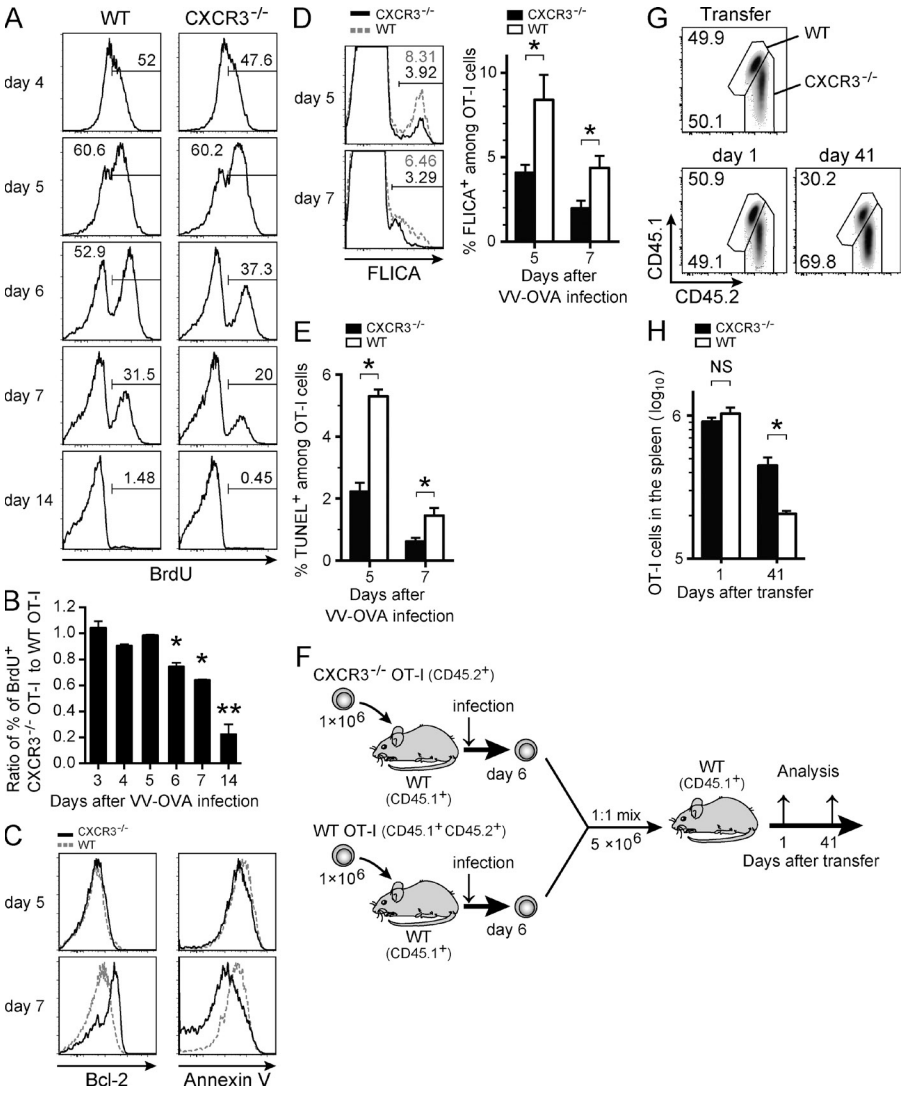

Figure 4. CXCR3$^{-/-}$ effector CD8$^+$ T cells show resistance to cell death in the late effector phase. (A–E) 1 d after transfer of mixed CXCR3$^{-/-}$ and WT OT-I cells, recipient mice were infected with VV-OVA as in Fig.1 B. (A) Recipient mice were i.p. injected with BrdU 24 h before sacrifice. Representative histograms gated on CXCR3$^{-/-}$ or WT OT-I cells in the spleen show BrdU incorporation. Numbers indicate the percentage of BrdU-positive population. (B) Ratio of percentage of BrdU-positive population of CXCR3$^{-/-}$ to WT OT-I cells. Data are shown as mean ± SEM. *, $P < 0.001$; **, $P < 0.0001$. (C–E) Apoptotic balance of CXCR3$^{-/-}$ and WT OT-I cells at days 5 and 7 after infection was evaluated by measuring percentage of Bcl-2$^+$ and annexin V$^+$ cells (C), pan-caspase activity (D), and TUNEL assay (E). Data are shown as mean ± SEM. *, $P < 0.05$. (F) CXCR3$^{-/-}$ and WT effector OT-I cells were generated in separate hosts and recovered from the spleen on day 6 after VV-OVA infection. A 1:1 mixture of CXCR3$^{-/-}$ and WT OT-I cells was transferred into naive hosts and contraction of both OT-I cell populations was compared. (G) Representative plots showing the percentage of CXCR3$^{-/-}$ (bottom) and WT (top) cells out of the total OT-I populations at days 1 and 41 after transfer. (H) Number of OT-I cells at days 1 and 41 after transfer. Data are shown as mean ± SEM. *, $P < 0.05$. Data represent three (A–C) or two (D–H) independent experiments (n = 3–4 per time point).

both cells had undergone similar division (Fig. 3 F). In addition, both memory OT-I cells showed similar redistribution and survival after transfer (Fig. 3, F and G; and unpublished data). Collectively, these data demonstrate that, despite phenotypic differences between CXCR3$^{-/-}$ and WT cells, the sustained numbers of CXCR3$^{-/-}$ memory CD8$^+$ T cells cannot be explained by their rates of homeostatic proliferation or their homing properties during the steady-state memory phase.

CXCR3$^{-/-}$ CD8$^+$ T cells primed in vivo are preferentially committed to become antiapoptotic and MPECs

Thus far, the data suggest that earlier events on CD8$^+$ T cell differentiation, after infection, may be the key to determining different amounts of memory formation. Therefore, we extended the BrdU approach, in which the proliferative responses of CXCR3$^{-/-}$ and WT effector CD8$^+$ T cells in the 24 h preceding sacrifice were measured during the early phase of infection. As shown in Fig. 4 (A and B), we observed consistent increases in BrdU incorporation for CXCR3$^{-/-}$ and WT effector CD8$^+$ T cells until day 5 after infection. Around the peak of expansion, however, increased frequencies of BrdU$^+$ cells were still observed in WT effector CD8$^+$ T cells, whereas those in the CXCR3$^{-/-}$ effector CD8$^+$ T cells decreased significantly (Fig. 4, A and B). This seems to contradict observation of preferential accumulation of CXCR3$^{-/-}$ memory CD8$^+$ T cells compared with WT counterparts. It should be noted that numbers of CXCR3$^{-/-}$ and WT CD8$^+$ T cells were indistinguishable until peak of expansion (Fig. 1 D). Because T cell accumulation results from a combination of cell death and proliferation, we hypothesized that CXCR3$^{-/-}$ effector CD8$^+$ T cells survive better than WT effector CD8$^+$ T cells at the peak of expansion as a result of small differences in number of effector CD8$^+$ T cells in the two groups. As anticipated, there was more apoptosis in WT compared with CXCR3$^{-/-}$ effector CD8$^+$ T cells as determined by expression of Bcl-2 and annexin V at day 7 (Fig. 4 C). A higher frequency of apoptosis in WT effector CD8$^+$ T cells was also confirmed by caspase activity and TUNEL assays (Fig. 4, D and E). To precisely compare contraction of CXCR3$^{-/-}$ and WT CD8$^+$ T cells, equal numbers of both effector OT-I

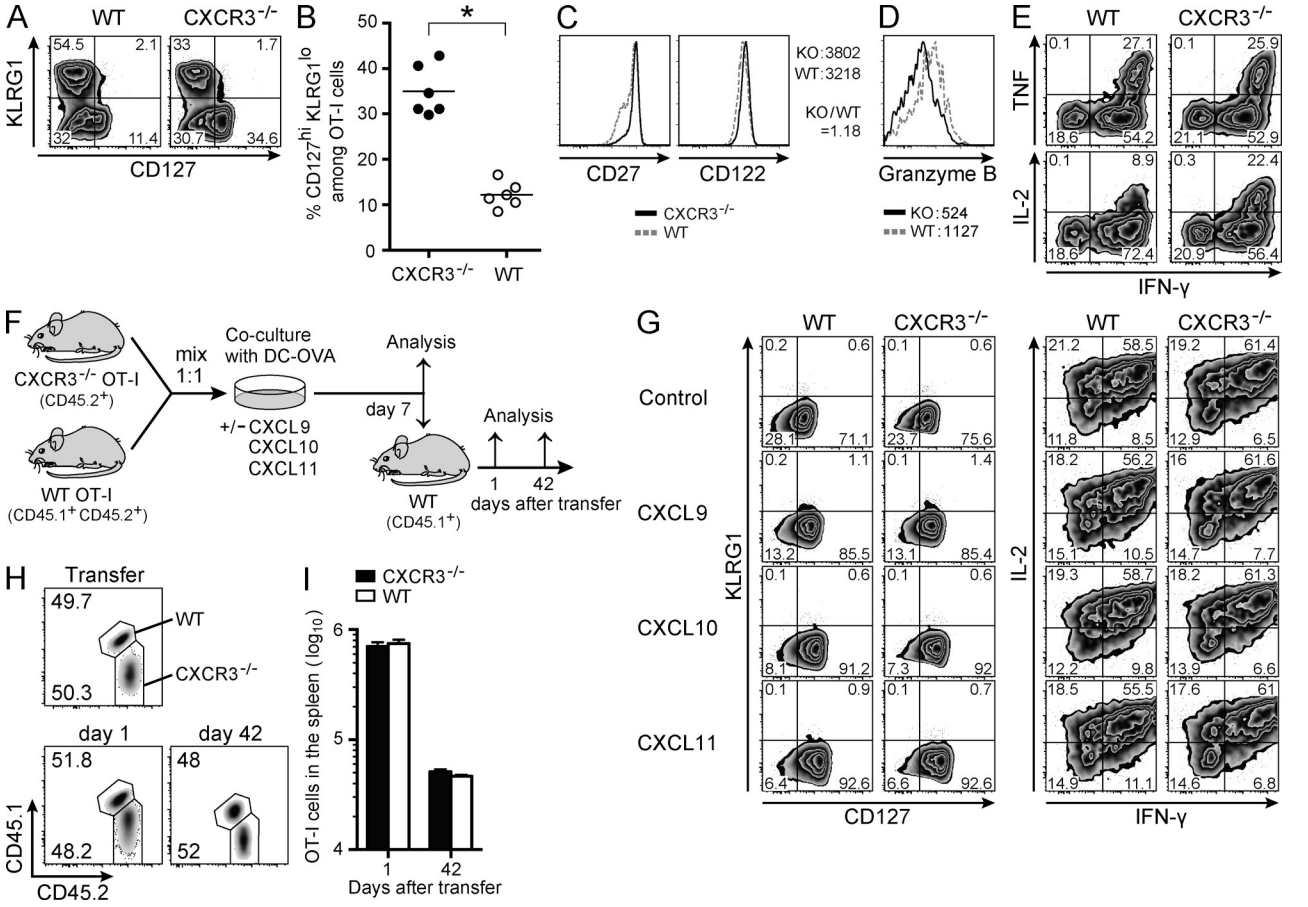

Figure 5. CXCR3 deficiency alters effector CD8+ T cell phenotype to MPECs in vivo. (A–E) 1 d after transfer of mixed CXCR3$^{-/-}$ and WT OT-I cells, recipient mice were infected with VV-OVA as in Fig.1 B. OT-I cells in spleen were analyzed at day 7 after infection. Data represent three independent experiments (n = 3–4 per time point). (A) Expression of CD127 and KLRG1. (B) Percentage of CD127^{hi} KLRG1^{lo} cells among OT-I cells. Bars represent mean. *, P < 0.0001. (C) Expression of CD27 and CD122. Numbers to the right of CD122 plots show MFI and MFI ratio of CXCR3$^{-/-}$ to WT. (D) Intracellular granzyme B expression. Numbers below granzyme B plots indicate MFI. (E) Intracellular TNF, IL-2, and IFN-γ production. (F) Naive CXCR3$^{-/-}$ and WT OT-I cells (mixed in a 1:1 ratio) were co-cultured with DC-OVA in the presence or absence of CXCR3 ligands (CXCL9, CXCL10, or CXCL11) for 7 d. (G) Phenotype and cytokine production profiles of OT-I cells on day 7. Representative data at 100 ng/ml ligand stimulation. (H and I) Cultured OT-I cells were transferred into WT mice. (H) Percentage of CXCR3$^{-/-}$ (bottom) and WT (top) cells in total OT-I populations at days 1 and 42 after transfer. (I) Number of in vitro–generated CTL at days 1 and 42 after transfer. Data are shown as mean ± SEM. (F–I) Data are representative of two independent experiments (n = 3).

cell types, primed in vivo, were transferred into the same recipient mice (Fig. 4, F–H). Consistent with previous results (Fig. 1 and Figs. S2–S4), CXCR3$^{-/-}$ effector cells exhibited more memory generation. These results indicate that the CXCR3$^{-/-}$ effector CD8$^+$ T cells proliferate well in the early expansion phase, but their proliferation later decreases and they are more resistant to apoptosis.

It is known that the effector CD8$^+$ T cell population can be subdivided into SLEC and MPEC populations; CD127^{lo} KLRG1^{hi} SLECs are considered more terminally differentiated with reduced longevity, whereas CD127^{hi} KLRG1^{lo} MPECs have a preferential ability to differentiate into a long-lived memory population (Joshi et al., 2007; Kaech and Wherry, 2007). It is also shown that SLECs divide longer than MPECs, and cells that continue to proliferate during late expansion contribute less to long-lived memory lineage (Sarkar et al., 2008). If this is so, CXCR3$^{-/-}$ effector CD8$^+$ T cells, in comparison with their WT counterparts, are more committed to becoming long-lived memory cells. This would also account for their attenuated contraction. To test this idea, we first compared the phenotype of CXCR3$^{-/-}$ and WT effector CD8$^+$ T cells. At day 7 after infection, CXCR3$^{-/-}$ effector CD8$^+$ T cells contained a higher frequency of CD127^{hi} KLRG1^{lo} CD27^{hi} MPECs and a lower frequency of CD127^{lo} KLRG1^{hi} CD27^{lo} SLECs, in comparison with their WT counterparts (Fig. 5, A–C). Predominant differentiation of CXCR3$^{-/-}$ cells into MPECs was also true for all lymphoid and nonlymphoid tissues determined (unpublished data). In addition to their phenotype, CXCR3$^{-/-}$ effector CD8+ T cells also exhibited various functional characteristics as MPECs, such as superior IL-2 but inferior granzyme B production compared with WT effector CD8$^+$ T cells (Fig. 5, D and E). This suggests that CD8$^+$ T cells, primed in the absence of CXCR3 in vivo, are programmed to become MPECs and have preferential longevity.

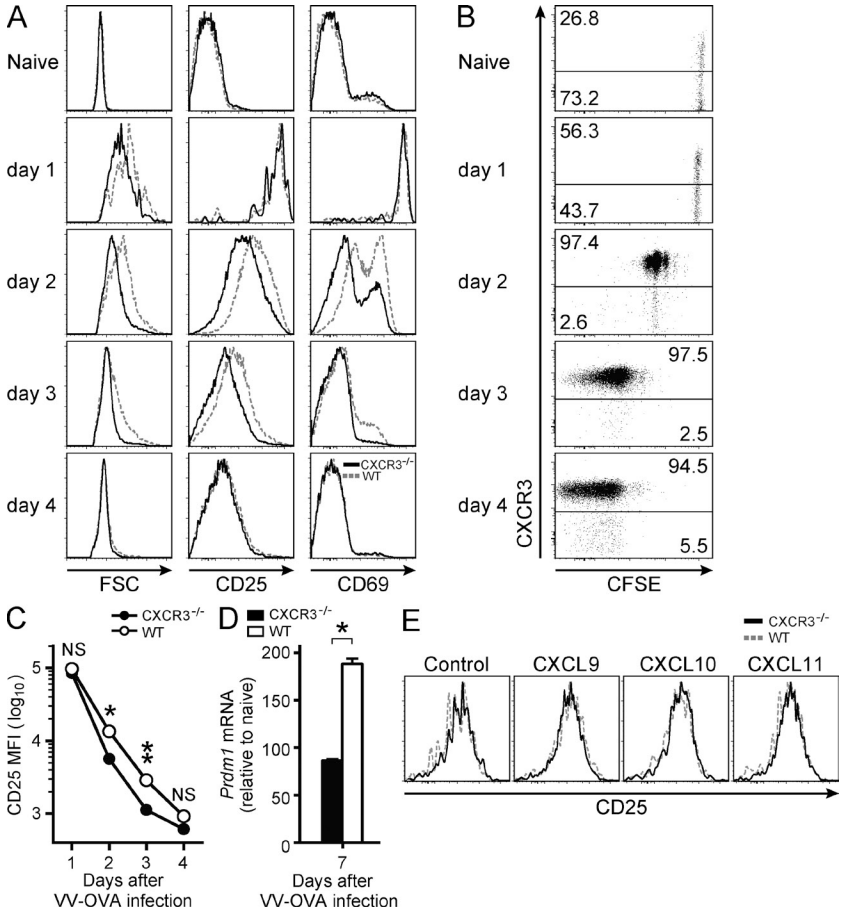

Figure 6. CXCR3$^{-/-}$ effector CD8$^+$ T cells exhibit shortened activation phenotype. (A–C) 1 d after transfer of mixed CXCR3$^{-/-}$ and WT OT-I cells (total ~1–3 × 10^6 cells), recipient mice were infected with VV-OVA as in Fig.1 B. (A) Surface expression of CD25 and CD69 and forward scatter (FSC) at the indicated times after infection. (B) Cell division (CFSE) and CXCR3 expression at indicated times after infection. (C) MFI of CD25 staining on OT-I cells at indicated times after infection. Data are shown as mean ± SEM. *, P < 0.0001; **, P < 0.005. (D) Relative *Prdm1* mRNA expression in OT-I cells was measured by quantitative RT-PCR at day 7 after infection. All data represent two independent experiments (n = 4 independent samples per time point) and are shown as mean ± SEM. *, P < 0.0001. (E) Mixed OT-I cells were stimulated by anti-CD3 and anti-CD28 antibodies, cultured in the presence and absence of CXCL9, CXCL10, and CXCL11 for 3 d, and stained for CD25. Representative histograms at 100 ng/ml CXCR3 ligand stimulation from two independent experiments are shown.

Recent research suggests that differential exposure to cytokines, including IL-2 and IL-12, during the early expansion phase alters cell fate decisions affecting SLEC or MPEC lineage (Joshi et al., 2007; Cui et al., 2009; Kalia et al., 2010; Pipkin et al., 2010). Because CXCR3 promotes lymphocyte migration to focus of inflammation, and CXCR3 deficiency is exclusively limited to one population of antigen-specific CD8$^+$ T cells in our experiments, it is reasonable to suggest that CXCR3$^{-/-}$ and WT CD8 T cells receive, quantitatively or qualitatively, different inflammatory signals and/or antigen presentation during the early expansion phase. It has been shown that CXCR3 might play a role as a costimulatory molecule. So it is possible that preferential differentiation of WT CD8$^+$ T cells into SLECs is a result of the intrinsic effect of CXCR3 signaling. To test this, we then examined whether priming and subsequent proliferation of both CD8$^+$ T cells in the same condition in vitro (without CXCR3-directed migration in vivo) would have an impact on their differentiation. Naive CXCR3$^{-/-}$ and WT OT-I cells were mixed together and stimulated in vitro with mature DCs loaded with OVA peptide (DC-OVA; Fig. 5 F). Strikingly, at day 7, in contrast to Fig. 5 A, we observed no differences in frequency of effector CD8$^+$ T cell subpopulation (MPECs vs. SLECs and percentage of IL-2$^+$ IFN-γ$^+$) between CXCR3$^{-/-}$ and WT effector OT-I cells (Fig. 5 G). This indicates that impact of CXCR3 on effector CD8$^+$ T cell fate decision is only observed when cells are primed in vivo. We also confirmed that skewed MPEC commitment is not a result of absence of intrinsic signals through CXCR3 on CD8$^+$ T cells because addition of CXCR3 ligands during proliferation in vitro had no impact on the phenotype characteristics of effector CD8$^+$ T cells (Fig. 5 G and unpublished data). Moreover, when we transferred in vitro–primed day-7 effector cells, CXCR3$^{-/-}$ OT-I cells now contracted at the same rate as WT OT-I cells in vivo (Fig. 5, H and I). Collectively, these results provide conclusive evidence that CXCR3 does alter effector CD8$^+$ T cell fate decision; CD8$^+$ T cells, primed in the absence of CXCR3 in vivo, are preferentially differentiated into MPECs, leading to the blunted contraction of effector CD8$^+$ T cells.

Shortened expression of CD25 on CXCR3$^{-/-}$ CD8$^+$ T cells

Previous studies demonstrate that strength and duration of inflammatory signals during the early expansion phase have a profound impact not only on divergent differentiation of effector subpopulations but also on the extent of CD8$^+$ T cell contraction (Badovinac et al., 2004; Joshi et al., 2007; Harty and Badovinac, 2008). Of these signals, IL-2 is recently reported to play a major role in effector CD8$^+$ T cell fate decision. Prolonged IL-2 signals and expression of CD25 (IL-2Rα) during the early expansion phase critically correlate with differentiation of CD8$^+$ T cells into SLECs (Kalia et al., 2010; Pipkin et al., 2010). We next examined very early events in CD8$^+$ T cell responses, including timing and duration of CD25 expression on CD8$^+$ T cells in vivo. 24 h after infection, both CXCR3$^{-/-}$ and WT OT-I cells displayed uniformly high expression of CD25 and CD69, indicating that

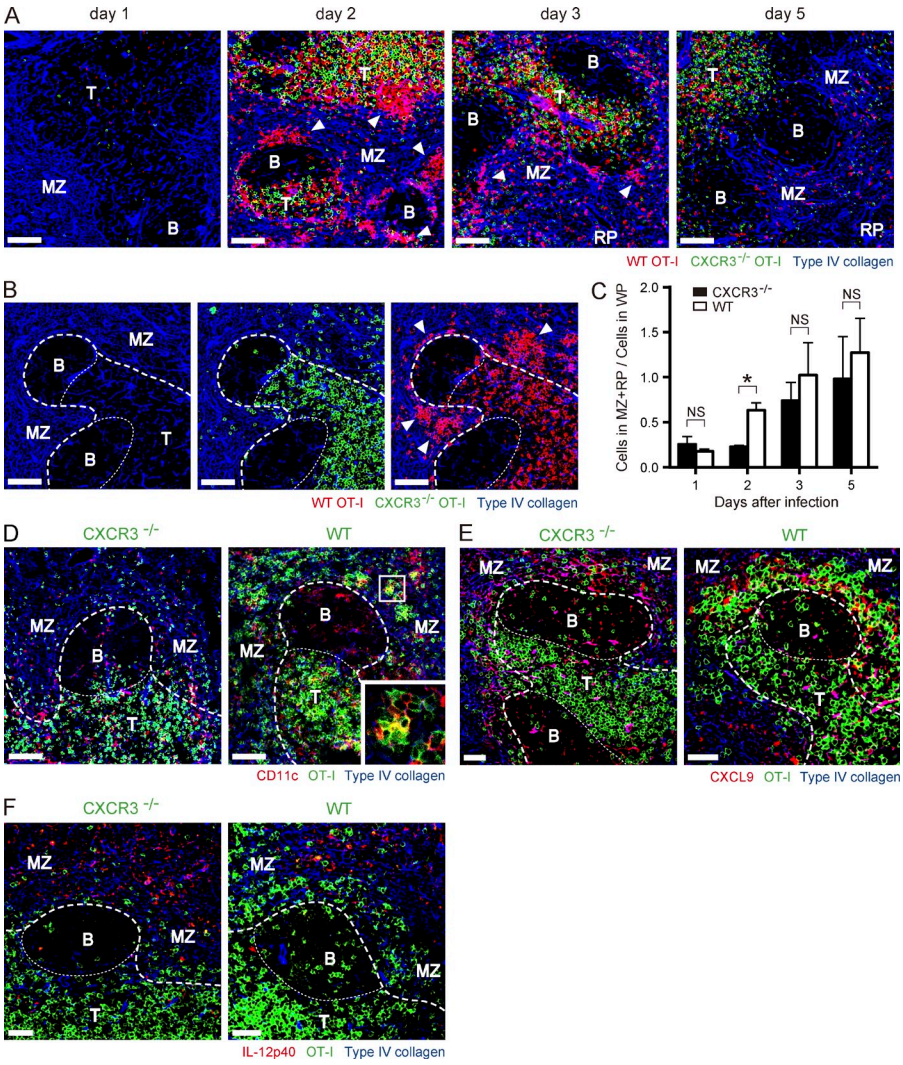

Figure 7. WT CD8⁺ T cells form clusters in the MZ of spleen early in the expansion phase. Spleen sections of mice that received a 1:1 mixture of CD45.1⁺ CXCR3$^{-/-}$ and CD90.1⁺ WT OT-I cells (~1–3 × 10^6 cells total) and were infected with VV-OVA were analyzed by immunofluorescent staining. The splenic compartments are represented as follows: T, T cell zone; B, B cell zone; bold dashed line, WP–RP border; thin dashed line, T cell–B cell zone border. Bars, 50 µm. (A and B) Sections were stained for CD90.1 (red, WT OT-I), CD45.1 (green, CXCR3$^{-/-}$ OT-I), and type IV collagen (blue). Arrows indicate clusters of WT OT-I cells. (B) Representative section from day 2 showing distribution CXCR3$^{-/-}$ and WT OT-I cells around T cell zone. (C) Ratio of OT-I cells in MZ/RP to those in WP. Data are shown as mean ± SEM. *, $P < 0.01$. (D) Sections were stained for CD11c (red), OT-I cells (green), and type IV collagen (blue) at day 2 after infection. (E) Sections were stained for CXCL9 (red), OT-I cells (green), and type IV collagen (blue) at day 2 after infection. (F) Sections were stained for IL-12p40 (red), OT-I cells (green), and type IV collagen (blue) at day 2 after infection. Data represent two (A–E) or three (F) independent experiments (n = 3–4 per time point).

the majority of cells were already activated (Fig. 6 A). It is important to note that a large fraction of WT OT-I cells strongly expressed CXCR3 at this point, even before cell division, suggesting a potential impact for this chemokine receptor on early CD8⁺ T cell responses (Fig. 6 B). By 48–72 h, when cells started division, CXCR3$^{-/-}$ OT-I cells downregulated CD25 and CD69 much faster than WT cells (Fig. 6, A and C). Along with CD25 and CD69 expression, CXCR3$^{-/-}$ OT-I cells showed reduced blastogenic response compared with WT cells (Fig. 6 A). Shortened expression of CD25 resulted in decreased Blimp-1 expression at later time points, indicating a decreased susceptibility of CXCR3$^{-/-}$ cells to IL-2 signaling (Fig. 6 D; Kalia et al., 2010). We considered the possibility that intrinsic signals through CXCR3 may prolong CD8⁺ T cell expression of CD25. To test this idea, CXCR3$^{-/-}$ and WT OT-I cells were stimulated in vitro in the presence of CXCR3 ligands. As shown in Fig. 6 E, CXCR3 ligands had no impact on duration of CD25 expression on CD8⁺ T cells during the early expansion phase. This suggests that CXCR3$^{-/-}$ CD8⁺ T cells are exposed to relatively weak inflammatory/antigenic stimuli in vivo, as compared with WT CD8⁺ T cells, and this leads to shortened expression of CD25 during early expansion followed by enhanced differentiation into MPECs.

Failure of acute cluster formation by CXCR3$^{-/-}$ CD8⁺ T cells

It is interesting that CXCR3$^{-/-}$ and WT CD8⁺ T cells exhibit differential activation as early as day 2 after infection, whereas both cells may acquire equivalent priming signals after infection because they both distribute in a similar way before infection (Fig. S1, B and C). Given that CXCR3 is expressed on almost all WT cells by this time (Fig. 6 B), CXCR3-dependent migration can account for these differences. Thus, we next investigated whether lack of surface expression of CXCR3 alters localization of antigen-specific CD8⁺ T cells after infection in spleen, a primary organ which initiates CD8⁺ T cell response after systemic infection with VV-OVA. Previous studies have shown that after systemic infection with LM-OVA, initial activation of antigen-specific CD8⁺ T cells in the spleen occurs at the borders of the B and T cell zones and in the marginal zones (MZs), followed by clear-cut formation of clusters with antigen-presenting cells (Khanna et al., 2007). After activation and proliferation, CD8⁺ T cells exit to the red pulp (RP) via bridging channels (Khanna et al., 2007). In the case of VV-OVA infection, both CXCR3$^{-/-}$ and WT CD8⁺ T cells were localized to T cell

zones in white pulp (WP) at 24 h after infection (Fig. 7 A). At 48 h, when high-level expression of CD25 remained on WT but not CXCR3$^{-/-}$ CD8$^+$ T cells (Fig. 6, A and C), WT CD8$^+$ T cells formed significant clusters at the MZ, whereas CXCR3$^{-/-}$ CD8$^+$ T cells rarely formed clusters and mainly existed in the T cell zone (Fig. 7, A–C). As already established (Khanna et al., 2007), antigen-specific CD8$^+$ T cells within the clusters were in close contact with CD11c$^+$ DCs (Fig. 7 D). DC–T cell interactions were also observed in the T cell zone (Fig. 7 D). Because CD8$^+$ T cells up-regulate CD25 while cells are undergoing brief serial contact with DCs, followed by stable DC–T cell interactions (Mempel et al., 2004), these data, together with those of Fig. 6 A, indicate that during T cell activation, WT cells have stable contact with DCs both at the clusters and T cell zone. CXCR3$^{-/-}$ cells, in contrast, are in contact only in the T cell zone. Cluster formation is probably not a result of superior clonal expansion of WT cells because both WT and CXCR3$^{-/-}$ cells divided equally at this time point (Fig. 6 B and unpublished data). Rather, the CXCR3 ligands CXCL9 and CXCL10 are mainly expressed in the MZ where CXCR3$^{-/-}$ cells fail to accumulate (Fig. 7 E and Fig. S6 A). This suggests that cluster formation of WT cells depends on CXCR3-mediated migration. It is known that DCs and macrophages in the MZ significantly express type I IFNs and IL-12 soon after infection, and this results in a highly inflamed microenvironment (Eloranta and Alm, 1999; Barchet et al., 2002; Louten et al., 2006; Kalies et al., 2008; Cui et al., 2009). Consistent with previous results, IL-12p40 and IFN-α were predominantly expressed in the MZ (Fig. 7 F; and Fig. S6, B and C). These findings provide strong support for the idea that migration of activated CD8$^+$ T cells to the MZ results in additional inflammatory stimuli, leading to prolonged expression of CD25 and accelerated differentiation toward SLECs. When cells underwent several divisions and down-regulated CCR7 (Fig. 6 B and Fig. S7 A), both WT and CXCR3$^{-/-}$ CD8$^+$ T cells were detected at the RP (Fig. 7, A and C). Together, these data show that CXCR3 influences the effector commitment of CD8$^+$ T cells via modulation of local distribution of activated cells during the early expansion phase.

DISCUSSION

The chemokine system has an essential role in optimal T cell response by coordinating localization and interaction of T cells and other immune cells (Bromley et al., 2008). The established view is that homeostatic chemokines, such as CCL19 and CCL21 (ligands of CCR7), play key roles in directing migration of both naive T cells and mature DCs to the draining lymph nodes where the adaptive immune response is initiated. Inflammatory chemokines, in contrast, are known to recruit full-fledged effector and memory T cells to inflamed nonlymphoid tissues where the pathogen first invades. Recent studies also show the role of inflammatory chemokines in priming CD8$^+$ T cells in which inflammatory chemokines, such as CCR4 and CCR5 ligands, secreted by licensed DCs, attract naive CD8$^+$ T cells to promote DC–T cell interactions (Castellino et al., 2006; Semmling et al., 2010). Our study extends these ideas by showing that in the absence of surface expression of CXCR3, activated CD8$^+$ T cells preferentially differentiate into MPECs and acquire longevity. We also found that CXCR3$^{-/-}$ CD8$^+$ T cells fail to cluster in MZ of spleen and exhibit shortened expression of CD25. These data suggest the novel idea that inflammatory chemokines have a substantial impact on CD8$^+$ T cell commitment to SLECs, rather than MPECs, by regulating localization of newly activated T cells within secondary lymphoid organs during early expansion.

Like the subcapsular sinus of lymph nodes, spleen MZ is an important site for capture of blood-borne pathogens and a gateway for lymphocytes entering the WP. The MZ is populated by B cells expressing high levels of surface IgM, DCs, and unique subsets of macrophages: ERTR-9–positive MZ macrophages and Moma-1–positive MZ metallophilic macrophages (Mebius and Kraal, 2005; Khanna and Lefrançois, 2008). These MZ macrophage subsets are known to play a pivotal role in filtering pathogens (Seiler et al., 1997; Oehen et al., 2002; Aichele et al., 2003). Moreover, both populations of MZ macrophages are the main producers of type I IFNs as well as IL-12 and respond quickly after virus infection (Eloranta and Alm, 1999; Louten et al., 2006; Cui et al., 2009). Likewise, CXCL9 is predominantly produced by macrophages and DCs in the MZ (Rabin et al., 2003; Liu et al., 2005; Rosenblum et al., 2010). These subsequently accelerate migration of conventional DCs to the T cell zone and cause aggregation of plasmacytoid DCs in the MZ, the latter of which further secrete type I IFNs (Barchet et al., 2002; Asselin-Paturel et al., 2005; Mebius and Kraal, 2005). Consequently, these unique innate cell populations synergistically enhance inflammatory milieu in the MZ. After entry of activated APCs to the WP, T cells are activated and up-regulate CXCR3 (as shown in this study) and this may allow them to traffic to a highly inflamed MZ, where cells acquire additional inflammatory signals and differentiate into SLECs. Overall, MZ is crucial, not only for sampling and transporting blood-borne pathogens and antigens but also for supporting differentiation of effector CD8$^+$ T cells by creating an inflammatory environment. In fact, MZ macrophages and MZ metallophilic macrophages can also be targets of LM and VV infection, respectively (Aichele et al., 2003; Muraille et al., 2005; Junt et al., 2008), and provoke antigen presentation and inflammation in the MZ. These findings support our propositional model that CXCR3 plays a specific role in directing migration of newly activated CD8$^+$ T cells to the MZ where they acquire further signals necessary to differentiation toward SLECs. In support of this idea, a recent paper has indicated that localization of antigen-experienced CD8$^+$ T cells in the spleen is linked to their differentiation status by showing that CD127^{hi} MPECs and memory cells are predominantly localized in the T cell zone, whereas CD127^{lo} SLECs and effector cells localize to the RP, which is closely connected to the MZ (Jung et al., 2010). Given the structural and cellular similarity of spleen and lymph node as T cell priming sites, it is interesting to examine whether CXCR3-mediated guidance influences

early commitment of effector $CD8^+$ T cell fates in models of localized infection.

It is particularly interesting that CXCR3-dependent migration of activated $CD8^+$ T cells to MZ takes place with maintained expression of CCR7. CCR7 is necessary to retention of T cells within the T cell zone, and down-regulation of both CCR7 and its ligands (CCL19 and CCL21) after infection causes exclusion of T cells from splenic WP. This allows these cells to enter the blood and peripheral tissues (Mebius and Kraal, 2005; Mueller et al., 2007). Our data show the relatively slow down-regulation of CCR7 on activated $CD8^+$ T cells and suggest that CCR7 may work as a temporal sequestrator, just as CD69 does in the lymph nodes. This maintains activated T cells within the WP while cells acquire signals essential to differentiation. A balance between expression levels of CXCR3 and CCR7 on activated $CD8^+$ T cells is probably a key factor in migratory force and subsequent fate decision. Our findings that preferential localization of WT $CD8^+$ T cells in the MZ occurs early after infection suggest that migratory cues mediated by CXCR3 modulate or override CCR7 cues when cells express CXCR3 at high levels. It should be noted that elevated expression of CXCR3 is exclusive to activated, but not naive, $CD8^+$ T cells. This may help selective recruitment of newly activated, but not noncognate, T cells to the MZ to maximize usage of inflammatory cytokines for optimal differentiation of effector $CD8^+$ T cells. Overall, these observations support a model that early $CD8^+$ T cell response is regulated by sequential involvement of chemokine receptors, such as CCR7 (before priming; gathering DCs and naive T cell), CCR4 and CCR5 (at priming; increasing DC–T cell interaction), and CXCR3 (after priming; enhancing effector differentiation).

It is known that TCR signaling is a trigger for up-regulation of CD25 (Kalia et al., 2010). Thus, the differential kinetics of CD25 expression, between $CXCR3^{-/-}$ and WT $CD8^+$ T cells early after infection, may be the result of not only an inflammatory stimuli gradient present in each microcompartment but also different amounts of antigen that T cells encounter in the context of MHC class I during priming. In the presence of high-dose antigen, antigen-specific $CD8^+$ T cells rapidly lose motility, up-regulate activation molecules including CD25, and undergo stable interactions with DCs (Henrickson et al., 2008). This may cause in situ visible cluster formation in the antigen-rich region. On the basis of this assumption, shortened CD25 expression on $CXCR3^{-/-}$ $CD8^+$ T cells may be a result of reduced strength and duration of TCR signaling and associated with failure of cluster formation. However, the amount of antigen available in vivo and strength of TCR signaling have an impact on the extent of T cell expansion (Kaech et al., 2002). Using recombinant vaccinia virus strains that produced high or low quantities of an OVA epitope, for example, it has been shown that $CD8^+$ T cell expansion after equivalent viral infections is proportional to epitope density (Wherry et al., 1999). Because $CXCR3^{-/-}$ and WT $CD8^+$ T cells underwent identical expansion in our own experiment, we believe that CXCR3-mediated proximity to inflammatory cytokines in the early expansion phase plays a dominant role in our experimental models. However, additional antigen exposure (TCR signaling) is another possible mechanism for the CXCR3-mediated fate decision in different models (locations and phases). Indeed, the accompanying article in this issue by Kohlmeier et al. demonstrates that additional antigen exposure at peripheral sites (the lungs) in the late effector phase of influenza infection has a significant impact on the $CXCR3^{-/-}$ $CD8^+$ T cell fate decision. Collectively, it appears that multiple mechanisms mediate CXCR3-mediated memory degeneration, such as inflammatory signals during early priming and additional antigen exposure during the late effector phase.

In terms of exposure to cytokines, one possible mechanism for differential CD25 expression between $CXCR3^{-/-}$ and WT $CD8^+$ T cells is the availability of IL-2. Duration, but not initiation, of CD25 expression on activated T cells is largely dependent on IL-2 availability (Kalia et al., 2010; Pipkin et al., 2010). IL-2 is known to be secreted directionally at the immune synapse, thus favoring CD25-expressing T cells in close proximity to APCs in either an autocrine or paracrine manner (Huse et al., 2006). On this basis, because maximum $CD8^+$ T cell production of IL-2 and cluster formation were observed at the same time point, CXCR3-mediated cluster formation may also enhance the impact of IL-2 on $CD8^+$ T cell differentiation into SLECs (Fig. 7, A-C; and Fig. S7 B). Together, CXCR3-mediated migration to the highly inflamed microcompartment may be important not only in acquiring additional inflammatory signaling but also in gathering activated T cells at the antigen-rich region where T cells receive additional autocrine and paracrine IL-2 signals.

Although our data support the idea that CXCR3-mediated migration to the MZ is responsible for effector $CD8^+$ T cell differentiation toward SLECs, the intrinsic effect of signaling through CXCR3 on this process must also be considered. Previous studies have addressed the role of chemokine receptors as a source of costimulatory and/or growth signals (Taub et al., 1996; Nanki and Lipsky, 2000; Real et al., 2004). In the case of CXCR3, earlier studies have shown that CXCR3 ligands stimulate T cell proliferation in vitro in MLR (Whiting et al., 2004). In addition, it has been shown that CXCR3 stimulation induces activation of TCR signaling molecules ZAP-70, LAT, and PLC-γ and these enhance T cell proliferation and chemotaxis (Dar and Knechtle, 2007; Newton et al., 2009). Moreover, signaling through CXCR3 induces activation of mTORC1 (Schwarz et al., 2009), which has recently been shown to be involved in memory $CD8^+$ T cell differentiation (Araki et al., 2009; Pearce et al., 2009). These important observations may explain enhanced differentiation of WT $CD8^+$ T cells toward SLECs as compared with $CXCR3^{-/-}$ $CD8^+$ T cells. Nevertheless, the descriptions of CXCR3-mediated intrinsic signals given in these in vitro studies do not match our current findings. For example, $CXCR3^{-/-}$ $CD8^+$ T cells in our study underwent equivalent proliferation and thus formed effector populations of

equivalent size as WT cells both in vivo and vitro, even in the absence of CXCR3-mediated co-stimulation. Importantly, in contrast to findings in vivo, when we stimulated $CD8^+$ T cells with CXCR3 ligands in vitro, we did not find any differences between $CXCR3^{-/-}$ and WT $CD8^+$ T cells in terms of phenotype, cytokine production, and survival after transfer. These important differences suggest that the intrinsic effects of CXCR3 observed in previous studies may play only a minor role in the overall $CD8^+$ T cell response in vivo. Thus, our in vivo data strongly support our proposed model that CXCR3-mediated altered distribution, rather than CXCR3-mediated intrinsic signals, plays a key role in the predominant generation of SLECs.

Because increased naive T cell precursor frequency results in nonphysiological T cell differentiation (Marzo et al., 2005; Badovinac et al., 2007), the data presented in this paper, using the adoptive transfer approach, needs careful evaluation. Timing of cluster formation by adoptive transfer TCR Tg cells, for example, was slightly different from that of endogenous antigen-specific $CD8^+$ T cells. In the adoptive transfer approach (transfer $\sim 10^6$ naive TCR Tg), peak cluster formation was evident 2 d after infection, followed by rapid scattering of Tg cells at the RP by day 5. This indicates egression of these cells from spleen. In contrast, Khanna et al. (2007) have shown that endogenous antigen-specific $CD8^+$ T cell clustering starts by day 2 and is still detectable at day 6. Although this may be a result of different kinetics with regard to $CD8^+$ T cell response to the particular pathogens used in these studies (VV versus LM), it may also be a result of increased precursor frequency accelerating $CD8^+$ T cell response (Badovinac et al., 2007; Obar et al., 2008). Furthermore, reduced numbers of TCR Tg cells ($\sim 10^4$) resulted in delayed cluster formation as well as peak CD25 expression by WT Tg cells (unpublished data). And regardless of the number of Tg cells transferred, prolonged expression of CD25 on WT, compared with $CXCR3^{-/-}$ $CD8^+$ T cells, is evident in all the experimental conditions determined and critical to the possibility of cells forming clusters (unpublished data). These results suggest that failure of $CXCR3^{-/-}$ $CD8^+$ T cells to form clusters is not caused by increased intraclonal competition with nonphysiological number of WT cells. Moreover, predominant memory formation of $CXCR3^{-/-}$ $CD8^+$ T cells was also observed under noncompetitive conditions (adoptive transfer approach using separate recipients; Fig. S2, C and D) or physiological precursor frequency (mixed BM chimera approach; Fig. S2, E–G). This supports our contention that, despite altered kinetics, precursor frequency is of minor importance to fated effector populations of $CXCR3^{-/-}$ and WT $CD8^+$ T cells.

Because heterologous expression of CXCR3 is evident on the functionally distinct memory $CD8^+$ T cell populations (Hikono et al., 2007), an important question raised by the current study is how the CXCR3-mediated fate decision during priming contributes to CXCR3 expression and to the functionality of memory $CD8^+$ T cells during memory phase. Based on our findings regarding the kinetics of CXCR3 expression on antigen-experienced $CD8^+$ T cells (Fig. 1), we speculated that expression of CXCR3 on memory $CD8^+$ T cells may not be closely linked to its expression during priming. When $CD8^+$ T cells are primed in the absence of CXCR3, cells receive relatively weak inflammatory signals and are differentiated preferentially into MPECs. In the case of WT $CD8^+$ T cells, nearly all activated $CD8^+$ T cells express CXCR3 after priming, followed by heterologous expression of CXCR3 on memory $CD8^+$ T cells: $CXCR3^{hi}$ with a stable phenotype and $CXCR3^{lo}$ with an activated phenotype (Fig. 1 and Fig. 6 B; Hikono et al., 2007). $CXCR3^{lo}$ memory $CD8^+$ cells have poor proliferative ability and, thus, decrease in number over time (Hikono et al., 2007). Taking these findings together, it is reasonable to conclude that the $CXCR3^{lo}$ memory $CD8^+$ T cell population is derived from $CXCR3^{hi}$ (capable of receiving strong inflammatory signals upon priming) but not $CXCR3^{lo}$ effector cells, although the mechanism responsible for the down-regulation of CXCR3 is unclear. Expression of CXCR3 remains on a subset of memory $CD8^+$ T cells that exhibit a stable phenotype ($CD27^{hi}$ $CD127^{hi}$ $CD43^{lo}$), which seemingly conflicts with our findings. Importantly, however, migration of activated ($CXCR3^+$) $CD8^+$ T cells to the MZ is not exclusive (Fig. 7), suggesting that $CXCR3^+$ (stable) memory $CD8^+$ T cells may be derived from $CXCR3^+$ effector $CD8^+$ T cells that remain within the T cell zone during priming. In fact, using classifications of Hikono et al. (2007), memory $CD8^+$ T cells generated in the absence of CXCR3 (primed only in the T cell zone) exhibit a highly stable phenotype ($CD27^{hi}$ $CD127^{hi}$) compared with their WT counterparts (Fig. 3). Although this classification fits nicely with our findings, the precise mechanisms regulating the dynamic expression of CXCR3 on antigen-experienced $CD8^+$ T cells, and the role of this mechanism in maintaining this T cell population, remains to be elucidated.

Overall, we conclude that CXCR3 is a key factor in influencing early programming of $CD8^+$ T cell differentiation. Because CXCR3 is rapidly expressed on almost all activated T cells, our findings strongly suggest that blockade of CXCR3-mediated relocalization of $CD8^+$ T cells to the hot spot during the early expansion phase is a promising approach for improving accumulation of fully functional antigen-specific memory $CD8^+$ T cells.

MATERIALS AND METHODS

Mouse and BM chimera. We purchased C57BL/6 mice from SLC, B6.SJL-*Ptprca* Pep3/BoyJ ($CD45.1^+$) and B6.Pl-*Thy1a*/Cy ($CD90.1^+$) mice from The Jackson Laboratory, and $Rag2^{-/-}$ OT-I mice from Taconic. B6.$Ccr5^{-/-}$ mice have been previously described (Murai et al., 2003). B6.$Cxcr3^{-/-}$ mice were provided by C. Gerard (Children's Hospital, Harvard Medical School, Boston, MA; Hancock et al., 2000). B6.$Cxcr3^{-/-}$ and B6.$Ccr5^{-/-}$ mice were crossed with $Rag2^{-/-}$ OT-I mice to generate $Rag2^{-/-}$ $CXCR3^{-/-}$ OT-I and $Rag2^{-/-}$ $CCR5^{-/-}$ OT-I mice, respectively. All mice were between 6 and 10 wk of age at the start of experiments. To generate mixed BM chimeras, B6 ($CD45.2^+$) mice were lethally irradiated (9 Gy) and subsequently injected i.v. with a total of 1×10^7 BM cells containing a mixture of $CXCR3^{-/-}$ ($CD45.1^+$) and B6 ($CD45.2^+$) in a 1:1 ratio. Mice were left at least 50 d before infection. All mice were used in accordance with the Animal Care Committee Guidelines of the Graduate School of Medicine, the University of Tokyo.

Virus, bacteria, and infection. Recombinant VV-OVA (Kedl et al., 2000) and LM-OVA (Pope et al., 2001) were obtained from P. Marrack (University of Colorado, Denver, CO) and H. Shen (University of Pennsylvania, Philadelphia, PA), respectively. Pathogens were propagated, titrated, and infected by intravenous injection to tail vein as previously described (Kedl et al., 2000; Pope et al., 2001; Kurachi et al., 2007). Unless otherwise described, we infected mice with VV-OVA at 2×10^6 PFU and LM-OVA at 5×10^4 CFU. For splenic LM-OVA titration, spleens were removed 3 d after high-dose (1×10^6–10^7 CFU) LM-OVA challenge, and 10-fold serial dilutions of homogenized spleen were cultured on brain-heart-infusion plates containing erythromycin.

Adoptive transfer and isolation of lymphocytes. For adoptive transfer of naive cells, $CD8^+$ T cells were isolated from spleen of naive $CXCR3^{-/-}$ or WT OT-I mice by CD8 negative selection (Miltenyi Biotec). The indicated number (1×10^4–10^6) of 1:1 mixed, or single OT-I cells, were transferred into nonirradiated naive recipient mice. After infection with VV-OVA or LM-OVA, major lymphoid and nonlymphoid organs were removed on the days indicated, and single cell suspensions were prepared as previously described (Kurachi et al., 2007). Unless otherwise stated in the relevant figure legends, all data in the manuscript is based on experiments conducted with spleen cells alone. RBCs in the cell suspensions were lysed using ammonium chloride. To transfer memory OT-I cells, $CXCR3^{-/-}$ and WT memory OT-I cell were generated in the two groups of mice. Spleen cells containing OT-I cells were isolated and further enriched for $CD8^+$ cells using CD8 negative selection. Before transfer, $CD8^+$ enriched spleen cells were analyzed to determine the proportion of $CXCR3^{-/-}$ or WT OT-I cells and were mixed carefully such that the cell mixture contained equal numbers of $CXCR3^{-/-}$ and WT OT-I cells or were transferred separately such that each recipient mouse received an equal number of OT-I cells ($1.9–2 \times 10^6$ cells).

Reagents, antibodies, and flow cytometry analysis. Recombinant IL-2, IL-4, GM-CSF, CXCL9, CXCL10, and CXCL11 were purchased from PeproTech. MHC class I peptide tetramers were purchased from MBL. OT-I epitope peptides ($OVA_{257-264}$: SIINFEKL) were obtained from Sigma-Aldrich. CpG ODN 1826 was purchased from Invitrogen. All antibodies used were purchased from BioLegend except for CD8a, KLRG1, IL-2, and CD43 (1B11; BD), CCR7 (eBioscience), anti–human granzyme B (GB12) and streptavidin–Alexa Fluor 488/647 (Invitrogen), anti-CXCL9 (R&D Systems), anti-CXCL10 (Santa Cruz Biotechnology, Inc.), and anti–IFN-α (Hycult Biotech). Assessment of caspase activity and DNA fragmentation was performed using FLICA Poly Caspases Assay kit (Immunochemistry Technologies) and APO-BrdU TUNEL Assay kit (Invitrogen). For intracellular cytokine staining, single cell suspension was incubated with or without 1 μM OT-I peptide in the presence of brefeldin A and IL-2 for 5 h at 37°C and stained using the Cytofix/Cytoperm kit (BD). Samples were analyzed on an LSRII (BD) and data were analyzed with FlowJo software (Tree Star).

In vivo CTL assay. The indicated number of $CXCR3^{-/-}$ and WT memory OT-I cells separately generated were adoptively transferred into naive $CD45.1^+$ mice. On the next day, a mixture of 5×10^6 unpulsed spleen cells labeled with 1 μM CFSE and 5×10^6 spleen cells pulsed with 1 μM OT-I peptide and labeled with 5 μM CFSE was administered intravenously to the indicated groups as well as a control group that received no memory cells. 4 h later, spleens were harvested, and the percentages of $CFSE^+$ cells that were $CFSE^{hi}$ and $CFSE^{lo}$ was assessed by flow cytometer. The percent specific killing was calculated as: $100 - (100 \times [(\%CFSE^{lo}/\%CFSE^{hi})/(\%CFSE^{lo}$ in no memory cells group/$\%CFSE^{hi}$ in no memory cells group)].

Measurement of proliferation by BrdU incorporation and CFSE. Mice were administered BrdU (200 μl of a 4 mg/ml solution in PBS) i.p. For assessment of acute proliferation in effector phase, mice were sacrificed 24 h after BrdU injection. For assessment of homeostatic proliferation in memory phase, mice were maintained on drinking water containing 0.8 mg/ml BrdU for 17 d. Single cell suspensions were stained with Abs to CD8a, TCR Vα2, CD45.1, and CD45.2, and BrdU incorporation was examined using a BrdU Flow kit (BD). In some proliferation assay, cells were labeled with 5 μM CFSE (Invitrogen) before transfer (Kurachi et al., 2007).

In vitro–generated CTL and effect of CXCR3 ligands in vitro. BM-derived DCs (BMDCs) were generated by culture of BM cells with GM-CSF and IL-4 as previously described (Badovinac et al., 2005). After purification by CD8 negative selection, naive splenic OT-I cells were co-cultured in vitro with BMDC pulsed with OT-I peptide (labeled at 10 nM) in the presence or absence of 0.1, 1, 10, 100, or 1,000 ng/ml CXCL9, CXCL10, and CXCL11 (PeproTech). 10 U/ml of recombinant human IL-2 was added to the culture medium after day 2. In the other experiments, OT-I cells were initially stimulated by 1 μg/ml of plate-bound anti-CD3 and anti-CD28 antibodies and cultured in the presence of CXCL9, CXCL10, and CXCL11. Proliferation, phenotype, and cytokine production were analyzed 3–7 d later.

Quantitative RT-PCR. RNA was isolated from $\sim 5 \times 10^5$ OT-I cells sorted by an ARIA cell sorter (BD). cDNA was synthesized using a High Capacity cDNA Reverse Transcription kit (Applied Biosystems). Real-time PCR was performed using an ABI 7500 instrument (Applied Biosystems) and Universal primer kit (Roche), and relative fold differences were calculated. All expression values were normalized to levels of the naive OT-I cells (WT or $CXCR3^{-/-}$). Primers used were as follows: *Prdm1* forward, 5′-GGCTCCACTACCCTTATCCTG-3′; *Prdm1* probe, 5′-GCTCACAG-3′; *Prdm1* reverse, 5′-TTTGGGTTGCTTTCCGTTT-3′; *Gapdh* forward, 5′-AGTATGACTCCACTCACGGCAA-3′; *Gapdh* probe, 5′-AACGGCACAGTCAAGGCCGAGAAT-3′; and *Gapdh* reverse, 5′-TCTCGCTCCTGGAAGATGGT-3′.

Immunofluorescence staining. Spleens were harvested and immersed in OCT medium (Sakura) and frozen in liquid nitrogen. For cytokine detection, 2–4-mm slices of spleen were incubated in PBS with brefeldin A for 6 h at 37°C before OCT immersion. 6-μm frozen sections were fixed in acetone, air dried, and stained with combinations of anti–CD45.1-FITC, anti–CD90.1-APC/biotin, anti–B220-biotin, anti-CXCL9, anti-CXCL10, anti–IL-12p40, anti–IFN-α, anti–CD11c-biotin, anti–sheep IgG–Alexa Fluor 488, anti–type IV collagen serum, anti–rabbit IgG–Alexa Fluor 555, anti–goat IgG–Alexa Fluor 555, and streptavidin–Alexa Fluor 488/647. Fluorescent images were obtained by a laser microscope (IX-70; Olympus) with a digital camera (EMCCD; Hamamatsu Photonics) and FluoView software (Olympus) and a fluorescent microscope (BZ-9000; Keyence). Distribution indexes were calculated as the ratio of [cells in RP + MZ] to [cells in WP].

Statistical analysis. Statistical significance was determined by Student's *t* test using Prism 5 (GraphPad Software). Significance was set as any p-value <0.05.

Online supplemental material. Fig. S1 shows a similar phenotype and distribution of donor $CXCR3^{-/-}$ and WT OT-I cells at the time of adoptive transfer. Fig. S2 shows that dominance of memory $CXCR3^{-/-}$ OT-I cells was confirmed until the very late memory phase in both dual and single transfer experiments and in mixed BM chimera experiment. Fig. S3 shows that CCR5 deficiency does not effect generation of memory $CD8^+$ T cells. Fig. S4 shows that an increased number of memory $CD8^+$ T cells in intact $CXCR3^{-/-}$ mice can provide enhanced protective immunity upon subsequent challenge. Fig. S5 shows that the surface expression of TCR and functional avidity of $CXCR3^{-/-}$ OT-I cells were similar to that of WT OT-I cells. Fig. S6 shows that CXCL10 and IFN-α were also predominantly expressed in the MZ. Fig. S7 shows the kinetics of CCR7 and CXCR3 expression and IL-2 production by OT-I cells in the early expansion phase. Online supplemental material is available at http://www.jem.org/cgi/content/full/jem.20102101/DC1.

We would like to thank Dr. M. Miller and F. Shand for critical proofreading and K. Morii, Y. Ishii, Dr. K. Kataoka, IMSUT FACS Core Laboratory, and the Center for NanoBio Integration (CNBI) at The University of Tokyo for flow cytometry and microscope facilities. We would also like to thank Y. Hosono, S. Iwashita, and C.

Kasahara for animal care and F. Marinho, S. Aoki, and S. Fujita for their excellent technical assistance.

This work was supported by The Ministry of Education, Culture, Sports, Science and Technology (MEXT) KAKENHI Grants-in-Aid for Young Scientists (B) 20790369 and 22790453 (M. Kurachi) and Grants-in-Aid for Scientific Research (B) 18209016 and 22390095 (K. Matsushima).

The authors declare that they have no competing financial interests.

M. Kurachi and K. Matsushima designed the experiments; M. Kurachi, J. Kurachi, F. Suenaga, T. Tsukui, K. Sugihara, and K. Kakimi carried out the experiments; M. Kurachi, J. Kurachi, S. Ueha, J. Abe, and M. Tomura analyzed the data, and M. Kurachi, S. Takamura, and K. Matsushima wrote the paper.

Submitted: 4 October 2010
Accepted: 24 June 2011

REFERENCES

Aichele, P., J. Zinke, L. Grode, R.A. Schwendener, S.H.E. Kaufmann, and P. Seiler. 2003. Macrophages of the splenic marginal zone are essential for trapping of blood-borne particulate antigen but dispensable for induction of specific T cell responses. *J. Immunol.* 171:1148–1155.

Araki, K., A.P. Turner, V.O. Shaffer, S. Gangappa, S.A. Keller, M.F. Bachmann, C.P. Larsen, and R. Ahmed. 2009. mTOR regulates memory CD8 T-cell differentiation. *Nature*. 460:108–112. doi:10.1038/nature08155

Asselin-Paturel, C., G. Brizard, K. Chemin, A. Boonstra, A. O'Garra, A. Vicari, and G. Trinchieri. 2005. Type I interferon dependence of plasmacytoid dendritic cell activation and migration. *J. Exp. Med.* 201:1157–1167. doi:10.1084/jem.20041930

Badovinac, V.P., B.B. Porter, and J.T. Harty. 2002. Programmed contraction of CD8(+) T cells after infection. *Nat. Immunol.* 3:619–626. doi:10.1038/ni804

Badovinac, V.P., B.B. Porter, and J.T. Harty. 2004. CD8+ T cell contraction is controlled by early inflammation. *Nat. Immunol.* 5:809–817. doi:10.1038/ni1098

Badovinac, V.P., K.A.N. Messingham, A. Jabbari, J.S. Haring, and J.T. Harty. 2005. Accelerated CD8+ T-cell memory and prime-boost response after dendritic-cell vaccination. *Nat. Med.* 11:748–756. doi:10.1038/nm1257

Badovinac, V.P., J.S. Haring, and J.T. Harty. 2007. Initial T cell receptor transgenic cell precursor frequency dictates critical aspects of the CD8(+) T cell response to infection. *Immunity*. 26:827–841. doi:10.1016/j.immuni.2007.04.013

Barchet, W., M. Cella, B. Odermatt, C. Asselin-Paturel, M. Colonna, and U. Kalinke. 2002. Virus-induced interferon α production by a dendritic cell subset in the absence of feedback signaling in vivo. *J. Exp. Med.* 195:507–516. doi:10.1084/jem.20011666

Bromley, S.K., T.R. Mempel, and A.D. Luster. 2008. Orchestrating the orchestrators: chemokines in control of T cell traffic. *Nat. Immunol.* 9:970–980. doi:10.1038/ni.f.213

Castellino, F., A.Y. Huang, G. Altan-Bonnet, S. Stoll, C. Scheinecker, and R.N. Germain. 2006. Chemokines enhance immunity by guiding naive CD8+ T cells to sites of CD4+ T cell-dendritic cell interaction. *Nature*. 440:890–895. doi:10.1038/nature04651

Cousens, L.P., R. Peterson, S. Hsu, A. Dorner, J.D. Altman, R. Ahmed, and C.A. Biron. 1999. Two roads diverged: interferon α/β– and interleukin 12–mediated pathways in promoting T cell interferon γ responses during viral infection. *J. Exp. Med.* 189:1315–1328. doi:10.1084/jem.189.8.1315

Crotty, S., R.J. Johnston, and S.P. Schoenberger. 2010. Effectors and memories: Bcl-6 and Blimp-1 in T and B lymphocyte differentiation. *Nat. Immunol.* 11:114–120. doi:10.1038/ni.1837

Cui, W., N.S. Joshi, A. Jiang, and S.M. Kaech. 2009. Effects of signal 3 during CD8 T cell priming: bystander production of IL-12 enhances effector T cell expansion but promotes terminal differentiation. *Vaccine*. 27:2177–2187. doi:10.1016/j.vaccine.2009.01.088

Curtsinger, J.M., J.O. Valenzuela, P. Agarwal, D. Lins, and M.F. Mescher. 2005. Type I IFNs provide a third signal to CD8 T cells to stimulate clonal expansion and differentiation. *J. Immunol.* 174:4465–4469.

Dar, W.A., and S.J. Knechtle. 2007. CXCR3-mediated T-cell chemotaxis involves ZAP-70 and is regulated by signalling through the T-cell receptor. *Immunology*. 120:467–485. doi:10.1111/j.1365-2567.2006.02534.x

Dufour, J.H., M. Dziejman, M.T. Liu, J.H. Leung, T.E. Lane, and A.D. Luster. 2002. IFN-gamma-inducible protein 10 (IP-10; CXCL10)-deficient mice reveal a role for IP-10 in effector T cell generation and trafficking. *J. Immunol.* 168:3195–3204.

Eloranta, M.L., and G.V. Alm. 1999. Splenic marginal metallophilic macrophages and marginal zone macrophages are the major interferon-alpha/beta producers in mice upon intravenous challenge with herpes simplex virus. *Scand. J. Immunol.* 49:391–394. doi:10.1046/j.1365-3083.1999.00514.x

Fadel, S.A., S.K. Bromley, B.D. Medoff, and A.D. Luster. 2008. CXCR3-deficiency protects influenza-infected CCR5-deficient mice from mortality. *Eur. J. Immunol.* 38:3376–3387. doi:10.1002/eji.200838628

Hancock, W.W., B. Lu, W. Gao, V. Csizmadia, K. Faia, J.A. King, S.T. Smiley, M. Ling, N.P. Gerard, and C. Gerard. 2000. Requirement of the chemokine receptor CXCR3 for acute allograft rejection. *J. Exp. Med.* 192:1515–1520. doi:10.1084/jem.192.10.1515

Harty, J.T., and V.P. Badovinac. 2008. Shaping and reshaping CD8+ T-cell memory. *Nat. Rev. Immunol.* 8:107–119. doi:10.1038/nri2251

Henrickson, S.E., T.R. Mempel, I.B. Mazo, B. Liu, M.N. Artyomov, H. Zheng, A. Peixoto, M.P. Flynn, B. Senman, T. Junt, et al. 2008. T cell sensing of antigen dose governs interactive behavior with dendritic cells and sets a threshold for T cell activation. *Nat. Immunol.* 9:282–291. doi:10.1038/ni1559

Hikono, H., J.E. Kohlmeier, S. Takamura, S.T. Wittmer, A.D. Roberts, and D.L. Woodland. 2007. Activation phenotype, rather than central– or effector–memory phenotype, predicts the recall efficacy of memory CD8$^+$ T cells. *J. Exp. Med.* 204:1625–1636. doi:10.1084/jem.20070322

Hokeness, K.L., E.S. Deweerd, M.W. Munks, C.A. Lewis, R.P. Gladue, and T.P. Salazar-Mather. 2007. CXCR3-dependent recruitment of antigen-specific T lymphocytes to the liver during murine cytomegalovirus infection. *J. Virol.* 81:1241–1250. doi:10.1128/JVI.01937-06

Huse, M., B.F. Lillemeier, M.S. Kuhns, D.S. Chen, and M.M. Davis. 2006. T cells use two directionally distinct pathways for cytokine secretion. *Nat. Immunol.* 7:247–255. doi:10.1038/ni1304

Intlekofer, A.M., N. Takemoto, C. Kao, A. Banerjee, F. Schambach, J.K. Northrop, H. Shen, E.J. Wherry, and S.L. Reiner. 2007. Requirement for T-bet in the aberrant differentiation of unhelped memory CD8$^+$ T cells. *J. Exp. Med.* 204:2015–2021. doi:10.1084/jem.20070841

Joshi, N.S., W. Cui, A. Chandele, H.K. Lee, D.R. Urso, J. Hagman, L. Gapin, and S.M. Kaech. 2007. Inflammation directs memory precursor and short-lived effector CD8(+) T cell fates via the graded expression of T-bet transcription factor. *Immunity*. 27:281–295. doi:10.1016/j.immuni.2007.07.010

Jung, Y.W., R.L. Rutishauser, N.S. Joshi, A.M. Haberman, and S.M. Kaech. 2010. Differential localization of effector and memory CD8 T cell subsets in lymphoid organs during acute viral infection. *J. Immunol.* 185:5315–5325. doi:10.4049/jimmunol.1001948

Junt, T., E. Scandella, and B. Ludewig. 2008. Form follows function: lymphoid tissue microarchitecture in antimicrobial immune defence. *Nat. Rev. Immunol.* 8:764–775. doi:10.1038/nri2414

Kaech, S.M., and E.J. Wherry. 2007. Heterogeneity and cell-fate decisions in effector and memory CD8+ T cell differentiation during viral infection. *Immunity*. 27:393–405. doi:10.1016/j.immuni.2007.08.007

Kaech, S.M., E.J. Wherry, and R. Ahmed. 2002. Effector and memory T-cell differentiation: implications for vaccine development. *Nat. Rev. Immunol.* 2:251–262. doi:10.1038/nri778

Kaech, S.M., J.T. Tan, E.J. Wherry, B.T. Konieczny, C.D. Surh, and R. Ahmed. 2003. Selective expression of the interleukin 7 receptor identifies effector CD8 T cells that give rise to long-lived memory cells. *Nat. Immunol.* 4:1191–1198. doi:10.1038/ni1009

Kalia, V., S. Sarkar, S. Subramaniam, W.N. Haining, K.A. Smith, and R. Ahmed. 2010. Prolonged interleukin-2Ralpha expression on virus-specific CD8+ T cells favors terminal-effector differentiation in vivo. *Immunity*. 32:91–103. doi:10.1016/j.immuni.2009.11.010

Kalies, K., P. König, Y.-M. Zhang, M. Deierling, J. Barthelmann, C. Stamm, and J. Westermann. 2008. Nonoverlapping expression of IL10, IL12p40, and IFNgamma mRNA in the marginal zone and T cell zone of the spleen after antigenic stimulation. *J. Immunol.* 180:5457–5465.

Kallies, A., A. Xin, G.T. Belz, and S.L. Nutt. 2009. Blimp-1 transcription factor is required for the differentiation of effector CD8(+) T cells and memory responses. *Immunity*. 31:283–295. doi:10.1016/j.immuni.2009.06.021

Kedl, R.M., W.A. Rees, D.A. Hildeman, B. Schaefer, T. Mitchell, J. Kappler, and P. Marrack. 2000. T cells compete for access to antigen-bearing antigen-presenting cells. *J. Exp. Med.* 192:1105–1113. doi:10.1084/jem.192.8.1105

Khanna, K.M., and L. Lefrançois. 2008. Geography and plumbing control the T cell response to infection. *Immunol. Cell Biol.* 86:416–422. doi:10.1038/icb.2008.22

Khanna, K.M., J.T. McNamara, and L. Lefrançois. 2007. In situ imaging of the endogenous CD8 T cell response to infection. *Science*. 318:116–120. doi:10.1126/science.1146291

Kohlmeier, J.E., S.C. Miller, J. Smith, B. Lu, C. Gerard, T. Cookenham, A.D. Roberts, and D.L. Woodland. 2008. The chemokine receptor CCR5 plays a key role in the early memory CD8+ T cell response to respiratory virus infections. *Immunity*. 29:101–113. doi:10.1016/j.immuni.2008.05.011

Kurachi, M., K. Kakimi, S. Ueha, and K. Matsushima. 2007. Maintenance of memory CD8+ T cell diversity and proliferative potential by a primary response upon re-challenge. *Int. Immunol.* 19:105–115. doi:10.1093/intimm/dxl127

Liu, L., M.K. Callahan, D. Huang, and R.M. Ransohoff. 2005. Chemokine receptor CXCR3: an unexpected enigma. *Curr. Top. Dev. Biol.* 68:149–181. doi:10.1016/S0070-2153(05)68006-4

Louten, J., N. van Rooijen, and C.A. Biron. 2006. Type 1 IFN deficiency in the absence of normal splenic architecture during lymphocytic choriomeningitis virus infection. *J. Immunol.* 177:3266–3272.

Marzo, A.L., K.D. Klonowski, A. Le Bon, P. Borrow, D.F. Tough, and L. Lefrançois. 2005. Initial T cell frequency dictates memory CD8+ T cell lineage commitment. *Nat. Immunol.* 6:793–799. doi:10.1038/ni1227

Mebius, R.E., and G. Kraal. 2005. Structure and function of the spleen. *Nat. Rev. Immunol.* 5:606–616. doi:10.1038/nri1669

Mempel, T.R., S.E. Henrickson, and U.H. Von Andrian. 2004. T-cell priming by dendritic cells in lymph nodes occurs in three distinct phases. *Nature*. 427:154–159. doi:10.1038/nature02238

Mueller, S.N., K.A. Hosiawa-Meagher, B.T. Konieczny, B.M. Sullivan, M.F. Bachmann, R.M. Locksley, R. Ahmed, and M. Matloubian. 2007. Regulation of homeostatic chemokine expression and cell trafficking during immune responses. *Science*. 317:670–674. doi:10.1126/science.1144830

Murai, M., H. Yoneyama, T. Ezaki, M. Suematsu, Y. Terashima, A. Harada, H. Hamada, H. Asakura, H. Ishikawa, and K. Matsushima. 2003. Peyer's patch is the essential site in initiating murine acute and lethal graft-versus-host reaction. *Nat. Immunol.* 4:154–160. doi:10.1038/ni879

Muraille, E., R. Giannino, P. Guirnalda, I. Leiner, S. Jung, E.G. Pamer, and G. Lauvau. 2005. Distinct in vivo dendritic cell activation by live versus killed Listeria monocytogenes. *Eur. J. Immunol.* 35:1463–1471. doi:10.1002/eji.200526024

Nakanishi, Y., B. Lu, C. Gerard, and A. Iwasaki. 2009. CD8(+) T lymphocyte mobilization to virus-infected tissue requires CD4(+) T-cell help. *Nature*. 462:510–513. doi:10.1038/nature08511

Nanki, T., and P.E. Lipsky. 2000. Cutting edge: stromal cell-derived factor-1 is a costimulator for CD4+ T cell activation. *J. Immunol.* 164:5010–5014.

Newton, P., G. O'Boyle, Y. Jenkins, S. Ali, and J.A. Kirby. 2009. T cell extravasation: demonstration of synergy between activation of CXCR3 and the T cell receptor. *Mol. Immunol.* 47:485–492. doi:10.1016/j.molimm.2009.08.021

Obar, J.J., K.M. Khanna, and L. Lefrançois. 2008. Endogenous naive CD8+ T cell precursor frequency regulates primary and memory responses to infection. *Immunity*. 28:859–869. doi:10.1016/j.immuni.2008.04.010

Oehen, S., B. Odermatt, U. Karrer, H. Hengartner, R. Zinkernagel, and C. López-Macías. 2002. Marginal zone macrophages and immune responses against viruses. *J. Immunol.* 169:1453–1458.

Pearce, E.L., M.C. Walsh, P.J. Cejas, G.M. Harms, H. Shen, L.-S. Wang, R.G. Jones, and Y. Choi. 2009. Enhancing CD8 T-cell memory by modulating fatty acid metabolism. *Nature*. 460:103–107. doi:10.1038/nature08097

Pham, N.-L.L., V.P. Badovinac, and J.T. Harty. 2009. A default pathway of memory CD8 T cell differentiation after dendritic cell immunization is deflected by encounter with inflammatory cytokines during antigen-driven proliferation. *J. Immunol.* 183:2337–2348. doi:10.4049/jimmunol.0901203

Pipkin, M.E., J.A. Sacks, F. Cruz-Guilloty, M.G. Lichtenheld, M.J. Bevan, and A. Rao. 2010. Interleukin-2 and inflammation induce distinct transcriptional programs that promote the differentiation of effector cytolytic T cells. *Immunity*. 32:79–90. doi:10.1016/j.immuni.2009.11.012

Pope, C., S.-K. Kim, A. Marzo, D. Masopust, K. Williams, J. Jiang, H. Shen, and L. Lefrançois. 2001. Organ-specific regulation of the CD8 T cell response to Listeria monocytogenes infection. *J. Immunol.* 166:3402–3409.

Rabin, R.L., M.A. Alston, J.C. Sircus, B. Knollmann-Ritschel, C. Moratz, D. Ngo, and J.M. Farber. 2003. CXCR3 is induced early on the pathway of CD4+ T cell differentiation and bridges central and peripheral functions. *J. Immunol.* 171:2812–2824.

Real, E., A. Kaiser, G. Raposo, A. Amara, A. Nardin, A. Trautmann, and E. Donnadieu. 2004. Immature dendritic cells (DCs) use chemokines and intercellular adhesion molecule (ICAM)-1, but not DC-specific ICAM-3-grabbing nonintegrin, to stimulate CD4+ T cells in the absence of exogenous antigen. *J. Immunol.* 173:50–60.

Rosenblum, J.M., N. Shimoda, A.D. Schenk, H. Zhang, D.D. Kish, K. Keslar, J.M. Farber, and R.L. Fairchild. 2010. CXC chemokine ligand (CXCL) 9 and CXCL10 are antagonistic costimulation molecules during the priming of alloreactive T cell effectors. *J. Immunol.* 184:3450–3460. doi:10.4049/jimmunol.0903831

Rutishauser, R.L., and S.M. Kaech. 2010. Generating diversity: transcriptional regulation of effector and memory CD8 T-cell differentiation. *Immunol. Rev.* 235:219–233.

Rutishauser, R.L., G.A. Martins, S. Kalachikov, A. Chandele, I.A. Parish, E. Meffre, J. Jacob, K. Calame, and S.M. Kaech. 2009. Transcriptional repressor Blimp-1 promotes CD8(+) T cell terminal differentiation and represses the acquisition of central memory T cell properties. *Immunity*. 31:296–308. doi:10.1016/j.immuni.2009.05.014

Sarkar, S., V. Kalia, W.N. Haining, B.T. Konieczny, S. Subramaniam, and R. Ahmed. 2008. Functional and genomic profiling of effector CD8 T cell subsets with distinct memory fates. *J. Exp. Med.* 205:625–640. doi:10.1084/jem.20071641

Schwarz, J.B.K., N. Langwieser, N.N. Langwieser, M.J. Bek, S. Seidl, H.-H. Eckstein, B. Lu, A. Schömig, H. Pavenstädt, and D. Zohlnhöfer. 2009. Novel role of the CXC chemokine receptor 3 in inflammatory response to arterial injury: involvement of mTORC1. *Circ. Res.* 104:189–200: 8p: 200. doi:10.1161/CIRCRESAHA.108.182683

Seiler, P., P. Aichele, B. Odermatt, H. Hengartner, R.M. Zinkernagel, and R.A. Schwendener. 1997. Crucial role of marginal zone macrophages and marginal zone metallophils in the clearance of lymphocytic choriomeningitis virus infection. *Eur. J. Immunol.* 27:2626–2633. doi:10.1002/eji.1830271023

Semmling, V., V. Lukacs-Kornek, C.A. Thaiss, T. Quast, K. Hochheiser, U. Panzer, J. Rossjohn, P. Perlmutter, J. Cao, D.I. Godfrey, et al. 2010. Alternative cross-priming through CCL17-CCR4-mediated attraction of CTLs toward NKT cell-licensed DCs. *Nat. Immunol.* 11:313–320. doi:10.1038/ni.1848

Slifka, M.K., and J.L. Whitton. 2001. Functional avidity maturation of CD8(+) T cells without selection of higher affinity TCR. *Nat. Immunol.* 2:711–717. doi:10.1038/90650

Takemoto, N., A.M. Intlekofer, J.T. Northrup, E.J. Wherry, and S.L. Reiner. 2006. Cutting edge: IL-12 inversely regulates T-bet and eomesodermin expression during pathogen-induced CD8+ T cell differentiation. *J. Immunol.* 177:7515–7519.

Taub, D.D., S.M. Turcovski-Corrales, M.L. Key, D.L. Longo, and W.J. Murphy. 1996. Chemokines and T lymphocyte activation: I. beta chemokines costimulate human T lymphocyte activation in vitro. *J. Immunol.* 156: 2095–2103.

Thapa, M., and D.J.J. Carr. 2009. CXCR3 deficiency increases susceptibility to genital herpes simplex virus type 2 infection: uncoupling of CD8+ T-cell effector function but not migration. *J. Virol.* 83:9486–9501. doi:10.1128/JVI.00854-09

Thompson, L.J., G.A. Kolumam, S. Thomas, and K. Murali-Krishna. 2006. Innate inflammatory signals induced by various pathogens differentially dictate the IFN-I dependence of CD8 T cells for clonal expansion and memory formation. *J. Immunol.* 177:1746–1754.

Wherry, E.J., K.A. Puorro, A. Porgador, and L.C. Eisenlohr. 1999. The induction of virus-specific CTL as a function of increasing epitope expression: responses rise steadily until excessively high levels of epitope are attained. *J. Immunol.* 163:3735–3745.

Wherry, E.J., V. Teichgräber, T.C. Becker, D. Masopust, S.M. Kaech, R. Antia, U.H. von Andrian, and R. Ahmed. 2003. Lineage relationship and protective immunity of memory CD8 T cell subsets. *Nat. Immunol.* 4:225–234. doi:10.1038/ni889

Wherry, E.J., S.-J. Ha, S.M. Kaech, W.N. Haining, S. Sarkar, V. Kalia, S. Subramaniam, J.N. Blattman, D.L. Barber, and R. Ahmed. 2007. Molecular signature of CD8+ T cell exhaustion during chronic viral infection. *Immunity*. 27:670–684. doi:10.1016/j.immuni.2007.09.006

Whiting, D., G. Hsieh, J.J. Yun, A. Banerji, W. Yao, M.C. Fishbein, J. Belperio, R.M. Strieter, B. Bonavida, and A. Ardehali. 2004. Chemokine monokine induced by IFN-gamma/CXC chemokine ligand 9 stimulates T lymphocyte proliferation and effector cytokine production. *J. Immunol.* 172:7417–7424.

Williams, M.A., and M.J. Bevan. 2007. Effector and memory CTL differentiation. *Annu. Rev. Immunol.* 25:171–192. doi:10.1146/annurev.immunol.25.022106.141548

Williams, M.A., A.J. Tyznik, and M.J. Bevan. 2006. Interleukin-2 signals during priming are required for secondary expansion of CD8+ memory T cells. *Nature*. 441:890–893. doi:10.1038/nature04790

Wirth, T.C., H.-H. Xue, D. Rai, J.T. Sabel, T. Bair, J.T. Harty, and V.P. Badovinac. 2010. Repetitive antigen stimulation induces stepwise transcriptome diversification but preserves a core signature of memory CD8(+) T cell differentiation. *Immunity*. 33:128–140. doi:10.1016/j.immuni.2010.06.014

Xiao, Z., K.A. Casey, S.C. Jameson, J.M. Curtsinger, and M.F. Mescher. 2009. Programming for CD8 T cell memory development requires IL-12 or type I IFN. *J. Immunol.* 182:2786–2794. doi:10.4049/jimmunol.0803484

Zhang, B., Y.K. Chan, B. Lu, M.S. Diamond, and R.S. Klein. 2008. CXCR3 mediates region-specific antiviral T cell trafficking within the central nervous system during West Nile virus encephalitis. *J. Immunol.* 180:2641–2649.